Journal of Electromyography and Kinesiology 22 (2012) 155–175

Contents lists available at SciVerse ScienceDirect

Journal of Electromyography and Kinesiology

journal homepage: www.elsevier.com/locate/jelekin

Review

Neuromuscular manifestations of viscoelastic tissue degradation following high and low risk repetitive lumbar flexion

M. Solomonow *

Musculoskeletal Disorders Research Laboratory, Bioengineering Division, Department of Orthopaedic Surgery, School of Medicine, University of Colorado, Denver, Aurora, CO 80045, USA

ARTICLE INFO

Article history:
Received 7 October 2010
Received in revised form 17 October 2011
Accepted 10 November 2011

Keywords:
Spine
Lumbar
Cumulative disorder
Cyclic loads
EMG
Cytokines
Creep
Stability
Viscoelastic tissues

ABSTRACT

Cumulative lumbar disorder is common in individuals engaged in long term performance of repetitive and static occupational/sports activities with the spine. The triggering source and of the disorder, the tissues involved in the failure and the biomechanical, neuromuscular, and biological processes active in the initiation and development of the disorder are not known. The hypothesis is forwarded that static and repetitive (cyclic) lumbar flexion-extension and the associated repeated stretch of the various viscoelastic tissues (ligaments, fascia, facet capsule, discs, etc.) causes micro-damage in their collagen fibers followed by an acute inflammation, triggering pain and reflexive muscle spasms/hyper-excitability. Continued exposure to activities, over time, converts the acute inflammation into a chronic one, viscoelastic tissues remodeling/degeneration, modified motor control strategy and permanent disability. Changes in lumbar stability are expected during the development of the disorder.

A series of experimental data from in-vivo feline is reviewed and integrated with supporting evidence from the literature to gain a valuable insight into the multi-factorial development of the disorder. Prolonged cyclic lumbar flexion-extension at high loads, high velocities, many repetitions and short in between rest periods induced transient creep/laxity in the spine, muscle spasms and reduced stability followed, several hours later, by an acute inflammation/tissue degradation, muscular hyper-excitability and increased stability. The major findings assert that viscoelastic tissues sub-failure damage is the source and inflammation is the process which governs the mechanical and neuromuscular characteristic symptoms of the disorder. A comprehensive model of the disorder is presented. The experimental data validates the hypothesis as well as provide insights into the development of potential treatment and prevention of the disorder.

Contents

* Address: Department of Orthopaedic Surgery, University of Colorado, Denver, HSC, RCI-N, 12800 E 19th Ave., Aurora, CO 80045, USA. Tel.: +1 303 724 0384.
E-mail address: moshe.solomonow@ucdenver.edu

1050-6411/$ - see front matter © 2011 Elsevier Ltd. All rights reserved.
doi:10.1016/j.jelekin.2011.11.008

1. Introduction

Cumulative trauma disorder (CTD), also known as repetitive exposure injury, is diagnosed with observation of severe pain, weakness, limited range of motion and stiffness/spasms in the musculature of the affected joint. The epidemiology identified the work force engaged in routine daily activities requiring prolonged cyclic (repetitive) flexion-extension as the most vulnerable population to CTD (Silverstein et al., 1986; Punnett et al., 1991; Punnett and Wegeman, 2004; Hoogendoorn et al., 2000; Andersson, 1997; Marras, 2000). Athletes on intense training programs are also a population at risk (Smoljanovic et al., 2009; Orchard et al., 2009). The epidemiology further asserts that individuals performing such prolonged cyclic activities while handling high loads, performing many repetitions at high movement velocities and over longer periods of time within the given day are at a high risk of exposure to CTD.

Attempts to identify a failure in a lumbar tissue/organ and the mode of failure as the source of the disorder were unproductive. Evidence of disc herniation, vertebral fracture, facet impingement or torn ligaments were absent in such patients. Furthermore, there were no biomechanical or neurophysiological data that confirm a relationship between prolonged exposure to cyclic flexion-extension and the disorder. Suspicions of muscle fatigue, genetic defects and psycho-social conditions as the major cause of CTD were expressed, without support of scientific evidence. A highly educated opinion pointed to the possibility of lumbar viscoelastic tissues (ligaments, discs, facet capsule, dorso-lumbar fascia, etc.) as the potential organs giving rise to the disorder once their cumulative tolerance is surpassed (Kumar, 2001, 2008). The literature provides fractions of data that may support such hypothesis. Woo et al. (1981, 1982, 1999) shown as far back as the early 1980s that cyclic loading of viscoelastic tissues result in micro-ruptures of some collagen fibers. This was recently repeated by Fung et al. (2009). If sufficient micro-ruptures are present in the ligaments, discs, facet, etc. an acute inflammation must follow to remove the damaged molecules in the first phase and repair the damage in the second phase (Leadbetter, 1990). Furthermore, since the lumbar ligaments, discs, fascia, etc. are also neurological tissues, having variety of afferents within, an inflammation may reduce their threshold and trigger muscular hyper-excitability (Cavanaugh et al., 2006, Bove et al., 2003; Dilley and Bove, 2008). The above fragments of data can provide a basis for formulating a complex hypothesis with systematic interaction of biomechanical, tissue properties, motor control as well as stability and function of the spine.

Overall, therefore, experimental evidence confirming the relationship of prolonged cyclic work to the cumulative disorder are missing; it is also not known which tissues fail and what is the mode of failure; what are the interactive relationships between the various neuro-musculoskeletal components; and finally, the implications of cyclic work and the disorder on lumbar stability and its motor control are absent.

The following multi-component hypothesis is therefore formulated:

Biomechanical component: Repetitive flexion of the lumbar spine will strain the viscoelastic tissues and induce creep (laxity) while also causing micro-damage to some collagen fibers if subjected to high loads, high velocities of strain, etc. Within several hours of rest post-work, a major recovery of the creep will take place while a residual creep associated with the non-functional, damaged collagen fibers will be observed until the healing phase of the inflammation is completed (see below).
Tissue biology component: Once the micro-damage exceeds a threshold level, an acute inflammation will be triggered, reaching a peak within several hours post work. The inflammation is bi-phasic, with initial removal of damaged collagen molecules and later repair of the damaged fibers leading to a full recovery.
Motor control component: Via afferents in the viscoelastic tissues, a reflexive activation of posterior lumbar musculature will be observed during the tissue's loading phase with superimposed spasms/injury potentials triggered by the micro-damage of some collagen fibers. With the developing laxity in the viscoelastic tissues during cyclic work, the intensity of muscular activation will diminish. Post work rest will allow the recovery of muscular activation intensity parallel to the recovery of the creep. The developing inflammation, however, will trigger muscular hyper-excitability that will last as long as the inflammation is present.
Stability: The gradually increasing creep/laxity in the viscoelastic tissues during cyclic work, together with the parallel decrease in reflexive muscular activation will leave the spine with diminished protection from instability, increasing the exposure to injury during late work and early in post work rest. With inflammation and its resulting muscular hyper-excitability, compensatory motor control will restore or over protect the spine from instability.

The complex hypothesis leads one to suspect that CTD is a syndrome rather than a disorder. Review of the following research will provide experimental confirmation of the biomechanical, tissue biology, motor control and stability components of the hypothesis. The outcome may provide valuable insight into the development of CTD, the tissues involved and the interaction of the various components. Furthermore, such insight may prove beneficial in formulating ergonomic measures to prevent the disorder and develop new

medical, chiropractic, physiotherapy and manipulative techniques to treat it effectively.

2. Methods

The preparation, instrumentation, protocols and data analysis presented below are for the convenience of the reader and a detailed account for each component is given in Hoops et al., 2007; Le et al., 2007; Lu et al., 2004, 2008; Navar et al., 2006; Eversull et al., 2001; Solomonow et al., 2001, 2008; Ben-Masaud et al., 2009; King et al., 2009; D'Ambrosia et al., 2010; Pinski et al., 2010.

2.1. Preparation

Adult cats, with an average weight of 4.0 ± 0.35 kg, were used in this study. They were anesthetized with 60 mg/kg chloralose, according to a protocol approved by the Institutional Animal Care and Use Committee. A superficial skin incision overlying the lumbar spine was made to expose the dorso-lumbar fascia, and an S-shaped stainless steel hook made of 1.5 mm diameter rod was applied around the supraspinous ligament mid-way between L_4 and L_5 spinal processes. The preparation was then positioned in a rigid stainless steel frame and the lumbar spine was isolated by means of two external fixators, which were applied to the L_1 and L_7 posterior processes, respectively. The external fixation was intended to limit the elicited flexion to the lumbar spine and to prevent interaction of thoracic and sacral and/or pelvic structures, but not to prevent any motion.

The number of cats for each test category (such as high loads, low loads, high frequency, low frequency, etc.) was first determined by power analysis to be $N = 8$ based on EMG variability which was the largest among all other variables (creep, cytokines, NNZs, etc.). Once testing reached $N = 6$, statistical analysis (see below) was performed to assess if significance was reached. If significance was not evident, additional cats were tested until significance was reached. This was done in order to minimize the use of animals. In general, N varied from a minimum of 6 to a maximum of 13.

2.2. Instrumentation

Three pairs of stainless steel fine wire EMG electrodes (inter-electrode distance: 3–4 mm) were inserted into the right L_{3-4}, L_{4-5}, and L_{5-6} multifidus muscles 6–8 mm laterally from the posterior spinal processes. A ground electrode was inserted into the gluteus muscle. Each electrode pair constituted the input to a differential EMG amplifier with a 110-dB common mode rejection ratio, a gain of up to 200,000, and a band-pass filter in the range of 6–500 Hz. The EMG was recorded with a sampling rate of 1000 Hz, and it was continuously monitored on an oscilloscope.

The S-shaped stainless steel hook inserted around the L_{4-5} supraspinous ligament was connected to the crosshead of the Bionix 858 Material Testing System (MTS, Minneapolis, MN), in which a load cell was placed in series with the loading system and monitored continuously along with the vertical displacement of the actuator. The load cell and displacement outputs of the Bionix 858 MTS were also sampled into the computer at 1000 Hz, along with the EMG signals.

Under such loading condition, the lumbar spine underwent anterior flexion-extension while straining the supraspinous, interspinous, and posterior longitudinal ligaments as well as the ligamentum flavum, facet capsule and dorsolumbar fascia. The discs in the lumbar spine were also deformed, expanding in their dorsal aspects while narrowing in their ventral aspects during the flexion phase. Overall, the neuromuscular response represents the reflexive activation of several lumbar viscoelastic components similar to those active during flexion-extension.

2.3. Protocol

A pre-load of 1 N was applied just prior to each single period of cyclic loading in order to produce a standard baseline across all preparations. Initially, three single cycles of 20 N peak load at 0.25 Hz were applied with a 10 min rest at no load between each cycle. This phase was performed for calibration, testing the system and to establish the normal neutral zones before cyclic loading. Following, a set of six 10 min cyclic loading periods at 20 N peak, each followed by 10 min rest was applied for a cumulative cyclic loading period of 60 min. The following recovery phase consisted of 7 h of rest at no load, during which single test cycles of 20 N peak load at 0.25 Hz were applied. The single cycles were applied 10, 30 and 60 min after the cyclic loading phase terminated and then once every hour. Overall, nine test cycles were applied during the 7 h recovery period. Fig. 1 depicts graphically the sequence of the cyclic loading with the single cycle tests before and after. Load, displacement and EMG from L_{3-4}, L_{4-5}, and L_{5-6} multifidus muscles were recorded throughout the protocol.

In order to assess the differences in response between high and low loads, the same protocol was repeated while changing the peak load from 20 to 40 N or 60 N. The 20–60 N range presented a physiological mild to heavy load with associated physiological strain range as determined earlier (Solomonow et al., 1998; Williams et al., 2000; Panjabi et al., 1982). Similarly, in order to assess the effect of flexion velocity, the frequency of the cyclic loading was changed from 0.25 to 0.5 Hz while keeping the same load and protocol. Furthermore, when the effect of the number of flexion-extension repetitions was of interest, the set of six 10 min loading followed by 10 min rest was modified to a set of three or nine 10 min loading followed by 10 min rest.

At the end of the 7 h recovery period, the supraspinous ligaments of the L_{3-4}, L_{4-5} and L_{5-6} were harvested from the specimen for cytokines analysis. For purposes of comparison, the supraspinous ligament of T_{10-11} from each preparation was also removed for analysis as self control since it was not subjected to the cyclic load or any associated motion. Comparison of lumbar ligaments to un-stimulated thoracic ligament as self control was scientifically advantageous. This, however, requires confirmation that baseline/un-stimulated cytokines level in different ligaments of the same specimen is approximately the same. For validation of this assumption, a control group of animals was tested and the validation was described elsewhere (King et al., 2009).

2.4. Data analysis

The analysis considered the recorded EMG, vertical displacement and cyclic load applied to the supraspinous ligament during the three pre-loading cycles, the six 10 min load/10 min rest loading period and the nine test cycles during the recovery period. Pro-inflammatory cytokines data was incorporated after harvesting the ligaments at the end of the 7 h rest and analyzing it.

2.4.1. Creep

The peak displacement of the first loading cycle of the first 10 min loading session at a given load and cyclic frequency was used to calculate the creep. This first peak displacement value was subtracted from each consecutive peak displacement starting from the second cycle and on and the difference was expressed as a percent of the first peak displacement according to the definition of creep. The creep values of the corresponding cycles of all the preparations exposed to the same loading condition were pooled and the mean (±SD) was calculated and plotted vs. time. During the

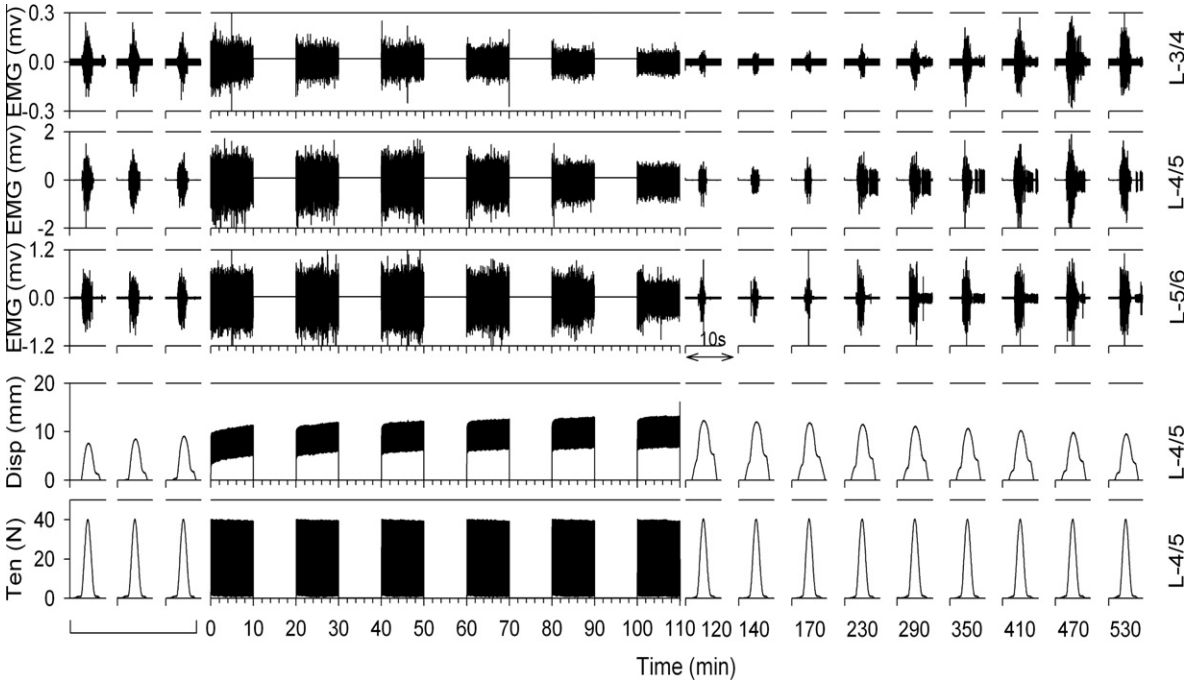

Fig. 1. Typical recording of the load, displacement and EMG from the three lumbar levels as collected from one preparation. The figure shows the three pre-loading test cycles used for normalization, the six 10 min loading sessions spaced by 10 min rest and the nine test cycles taken during the 7 h recovery/rest period.

recovery period, the creep of each test cycle was calculated and pooled with the respective cycles of the other preparation and the mean (±SD) calculated and also plotted vs. time. Full protocols are given in Hoops et al., 2007; Le et al., 2007; Lu et al., 2004, 2008; Navar et al., 2006.

2.4.2. EMG

A 4 s window of EMG corresponding to the first cycle of 0.25 Hz (or a 2 s window for loading frequency of 0.5 Hz) was taken at the beginning of the loading period and every minute thereafter. The EMG within each window was full wave rectified and integrated over the 4 s (or 2 s) period and normalized with respect to the first cycle of the first loading session to yield the Normalized Integrated EMG (NIEMG). The NIEMGs of all preparations subjected to the same peak load at the respective window were pooled, and the mean (±SD) were calculated and plotted on an NIEMG vs. time plot for each of the test categories used (e.g. peak loads, number of repetitions, frequencies, etc.). The NIEMG was selected to eliminate any inter-preparation differences such as size, electrode location and contact in the tissue. The NIEMG will also smooth the raw EMG to some extent, allowing better representation of the overall muscular activity over time. Full protocols are given in Hoops et al., 2007; Le et al., 2007; Lu et al., 2004, 2008; Navar et al., 2006.

2.4.3. Neuromuscular Neutral Zones

The motor control component of stability was assessed by the Neuromuscular Neutral Zones (NNZ) which was first defined in earlier reports (Eversull et al., 2001; Solomonow et al., 2001, 2008; Ben-Masaud et al., 2009). Each cycle was analyzed in a 5 s window including 0.5 s before and 0.5 s after the 4-s cycle (0.25 Hz). EMG threshold analysis was performed as follows: the first 0.5 s of each EMG record, which was before the initiation of movement by the actuator, was used as a benchmark for baseline EMG signal level. The mean absolute value (MAV) of this baseline was calculated: the signal recorded from each lumbar level was full wave rectified and smoothed with a 0.2 s moving average filter (every 10 points) to yield the EMG-MAV. The filter was centered on the window under consideration in order to prevent any time lags from affecting the data. After the initial 0.5 s period, any point along the absolute value (full wave rectified) of the EMG during the given cycle that exceeded three times the baseline MAV was denoted as the threshold of activity in that channel. The corresponding tension and displacement values during the stretch phase (increasing load) of the cycle were recorded as the TNNZ (Tension Neuromuscular Neutral Zone) and DNNZ (Displacement Neuromuscular Neutral Zone) threshold values, respectively, for that particular trial and lumbar level. Similarly, as the EMG dropped below the three times baseline MAV threshold in the release phase (decreasing load) of the cycle, the corresponding tension and displacement were recorded as the TNNZ and DNNZ thresholds, respectively, of cessation of activity. Fig. 7 shows the definitions described here in their graphical version. This automatic procedure was visually supervised to ensure that any unexpected signal artifacts were not detected as thresholds. Furthermore, in cases where the EMG traces included spasms along the baseline, or the EMG discharge during the flexion-extension was below three times baseline, the thresholds were determined visually.

The DNNZ and TNNZ from corresponding cycles during the recovery period for each of the preparations were pooled across lumbar level, and the mean (±SD) were calculated and plotted as a function of time. The DNNZ and TNNZ of the three cycles applied before cyclic loading was initiated were averaged for each preparation to yield a mean and SD, and then pooled with those of the other preparations to use as the pre-loading NNZ baselines.

The peak MAV (PMAV) of the first three single cycle recorded pre- loading was used as a normalization value for the peak MAV recorded in the test cycles of the same preparation during the 7 h recovery period. A single peak value was determined for each cycle. The normalized values of all the preparations were pooled, and the mean (±SD) was calculated and plotted as normalized peak MAV vs. time to assess whether the contraction level increased or decreased because of cyclic loading.

EMG Median Frequency (MF) was calculated for each single-cycle test in order to identify changes in motor unit recruitment

(Solomonow et al., 1990). A 500 msec window, centered at the peak load of each cycle, within which EMG was approximated as a stationary signal, was zero-padded on both sides. A Tukey window was applied to the zero-padded data, the power spectral density of the signal in this window was found via the fast Fourier transform, and the MF, defined as the frequency that divides the area under the power spectral density in half, was calculated. The MF values of all corresponding time points and lumbar levels were pooled and plotted as mean MF vs. recovery time with the mean of the pre-loading MF as baseline.

2.4.4. Cytokines analysis

(See full protocols in Solomonow et al., 2003; King et al., 2009; D'Ambrosia et al., 2010; Pinski et al., 2010) RNA extraction and preparation of cDNA was the first phase. Ligaments were flash frozen in liquid nitrogen, stored at −80 °C then powdered in a laboratory ball mill (Mikro-Dismembrator S, Sartorious BBI Systems, Inc., Bethlehem, PA). RNA was extracted and purified from the powdered ligaments using the RNeasy Lipid Tissue Mini Kit according to manufacturer's directions (QIAGEN, Valencia, CA). The procedure included an on-column DNase step. The average concentration, purity, and yield of RNA extracted from all ligaments were 120 ng/μl, 2.07 (λ 260/280 nm), and 3.7 μg, respectively. Complementary DNA (cDNA) was prepared from 1 μg of RNA isolated from each sample using the HC cDNA RT kit with RNase inhibitor (Applied Biosystems, Foster City, CA).

Quantitative real-time PCR was the second phase. Expression of gene targets was measured using real-time RT-PCR. Primers and probes for IL1-β, IL-6, IL-8, TNF-α, and TGF-β were designed with the assistance of the Primer Express sequence detection software (Applied Biosystems, Foster City, CA). TaqMan probes (Applied Biosystems, Foster City, CA) with 5′-label of 6-carboxy fluorescein and 3′-label of 6-carboxy-tetramethylrhodanline. Fifty micro-liter reaction mix containing TaqMan Universal Master Mix, forward and reverse primers, probes, RNase-free water, and 1 μg of the template cDNA was amplified for each target using an ABI prism 7500 sequence detector (Applied Biosystems, Foster City, CA) with an initial melt at 95 °C for 10 min followed by 40 cycles of amplification at 95 °C for 15 s and 60 °C for 1 min. Real-time data acquisition and analysis were performed using Ct values in which mRNA levels for each gene were normalized to the corresponding expression levels of glyceraldehyde-3-phosphate dehydrogenase (GAPDH). A standard curve was generated for each gene using the fluorescent data from the 10-fold serial dilutions of the amplicon that matched the specified primers. The standard curves for each gene did not differ significantly between experiments meaning that normalized values could be compared directly between experiments.

2.5. Statistics

2.5.1. NIEMG and displacement vs. time during recovery

A two way analysis of variance (ANOVA) was performed to assess the effect of time post-loading, load magnitude, number of repetitions, loading frequency and in-between rest (independent variable) on the recovery of the NIEMG and displacement. A post-Hoc test was performed to determine effect of the specific protocol variable (magnitude, rest, frequency, etc.) on the NIEMG and displacement for each of the three lumbar levels. Significance was set to <0.05 for all statistical tests.

2.5.2. Neuromuscular Neutral Zones

The data was divided into three lumbar levels (L_{3-4}, L_{4-5}, and L_{5-6}) for statistical analyses. The DNNZ, TNNZ, and peak EMG-MAV and MF data were visually inspected for normality. If a distribution did not appear normal, an appropriate data transformation was applied. Two-way repeated measures ANOVAs were used to test for differences in the stretch and relaxation phases and changes over time of the DNNZ and TNNZ. The independent variables included time (pre-cyclic loading and recovery times) and loading phase (stretch and relaxation). All higher order factorial terms were included in the statistical models to test for interaction of the independent variables. One-way repeated measures ANOVAs were used to test for changes over time in the EMG-based variables. The independent variables included time (pre-cyclic loading and recovery times) and the dependent variables were normalized peak MAV and MF. Upon determining a significant interaction or main effect, pair-wise comparisons were performed using a Student's t test. Level of significance for all tests was set as $p = 0.05$.

2.5.3. Cytokines

Cytokine expression levels (IL-1β, IL-6, IL-8, TGF-β, and TNF-α) for L_{3-4}, L_{4-5}, and L_{5-6} were divided by the cytokine expression levels in the T_{10-11} reference ligament harvested from the same cat for normalization. Comparison between the different loading rates was accomplished using a two-way mixed-model ANOVA where loading rate (0.25 and 0.5 Hz) and vertebral level (L_{3-4}, L_{4-5}, and L_{5-6}) were fixed variables and specimen was a random variable. Upon significant interactions or main effects in both tests, post hoc analyses were performed using a Student t tests to delineate statistically significant effects. All data were visually inspected for a normal distribution and an appropriate data transformation was applied if necessary. Prior to data transformation, the highest and lowest values from each loading rate × vertebral level grouping were removed before any analyses were performed. Level of significance was set at 0.05.

Similar protocol was used to assess differences between load magnitudes of 20 and 60 N.

2.6. Modeling

All models consisted of exponential components since they represent the classical response to viscoelastic materials such as the ligaments, discs, etc. involved in these experiments (Solomonow et al., 1999, 2000).

2.6.1. Creep

The creep during the loading periods followed an exponential model:

$$\mathrm{CREEP}(t) = C_0 + C_L(1 + e^{-t/T_2})$$

where CREEP(t) is the calculated creep as a function of time (mm), C_0 is the elastic component amplitude of creep (in percent), C_L is the viscoelastic component amplitude (in percent), T_2 is the time constant (min), and t is time.

The model for the creep during the recovery period is:

$$\mathrm{CREEP}(t) = C_0 + R + (C_L - R)e^{-t/T_3}$$

where C_0 is the elastic component amplitude of displacement (in percent), C_L is the viscoelastic component amplitude at the end of loading (in percent), R is the residual creep at the end of recovery (in percent), and $T3$ is the recovery time constant (min).

The parameters for all models fitted were obtained by using the Marquardt–Levenberg nonlinear regression algorithm.

2.6.2. Electromyogram (NIEMG)

For the NIEMG during the loading period:

$$\mathrm{NIEMG}(t) = Ae^{-t/T_1} + \mathrm{NIEMGss}$$

where A is the exponential component initial amplitude (unitless), $T1$ is the exponential decay time constant (min), NIEMGss is the steady-state NIEMG amplitude (unitless), and t is time.

For the NIEMG during the recovery period, the model format was:

$$\mathrm{NIEMG}(t) = E(1 - e^{-t/T_4}) + tBe^{-t/T_5} + C(t - T_d)e^{-(t-T_d)/T_6} + \mathrm{NIEMG}_0$$

where $E(1 - e^{-t/T_4})$ represents the steady-state recovery component, tBe^{-t/T_5} is a transient hyperexcitability component, $C(t - T_d)e^{-(t-T_d)/T_6}$ the delayed transient hyper-excitability. This term becomes functional only for $t \geqslant T_d$. NIEMG_0 represents the residual response at the end of the loading period (unitless). In this model, the constraint of $E + \mathrm{NIEMG}_0 = 1$ is used to ensure that full recovery results in a normal (unity) response. E, B, and C are unitless. T_4, T_5, T_6, and T_d are expressed in minutes.

The second and third terms, therefore, are transient features that first increase and then reverse (decrease) over time to finally arrive to near zero as the effect of hyper-excitability diminishes with rest. Furthermore, the third term, which represents the delayed hyper-excitability, becomes effective only after $t \geqslant T_d$; that is, the effect of this term is null until recovery time exceeds T_d. Overall, the model provides a unique prediction of the NIEMG at any given time during a rest period following a cyclic loading period.

The parameters for the models fitted were also obtained by using the Marquardt–Levenberg nonlinear regression algorithm.

2.6.3. Neuromuscular Neutral Zones

The mean ± SD values of the DNNZ, TNNZ, peak MAV, and MF during recovery for each lumbar level were also fit with exponential-based models, as they represent the classical response of viscoelastic tissues (Solomonow et al., 2000).

The time-course of the DNNZ thresholds during the stretch phase and relaxation phase of the test cycles during the recovery period were described by:

$$\mathrm{DNNZ}(t) = D_0 + (t - T_r)D_L e^{-(t-T_r)/T_1} + D_m e^{-(t-T_r)/T_1}$$

For all t values over 7 h recovery, where D_0 is the intercept of the displacement (mm), D_L affects the rise amplitude (mm/s), D_m is the amplitude of the decay dominating the end of the recovery period (mm), $(t - T_r)D_L e^{-(t-T_r)/T_1}$ allows for a transient rise at the beginning of the recovery period, T_1 affects the rates of rise and fall (s), T_2 is the exponential time-constant of the decay that dominates the end of the recovery period (min).

As noted above, the model was evaluated from the time point of 120 to 530 min, which constitutes the 7 h of recovery post-cyclic loading.

The time-course of the TNNZ thresholds during the stretch phase and relaxation phase of the test cycles during the recovery period were described by:

$$\mathrm{TNNZ}(t) = T_0 + (t - T_r)T_L e^{-(t-T_r)/T_3} + T_M e^{-(t-T_r)/T_4}$$

For all t values over 7 h recovery, where T_0 is the intercept of the tension (N), T_L affects the rise amplitude (N/s), T_M is the amplitude of the decay dominating the end of the recovery period (N), $(t - T_r)D_L e^{-(t-T_r)/T_3}$ allows for a transient rise at the beginning of the recovery period, T_3 affects the rates of rise and fall (s), and T_4 is the exponential time-constant of the decay that dominates the end of the recovery period (min).

2.6.4. Peak MAV of the EMG

The time-course of the peak MA V during the recovery period were described by:

$$\text{Peak MAV}(t) = \begin{cases} P_0 + P_L e^{-(t-T_r)/T_5} + P_M(1 - e^{-(t-T_r)/T_6}), & t < T_d \\ P_0 + P_L e^{-(t-T_r)/T_5} + P_M(1 - e^{-(t-T_r)/T_6}) \\ \quad +(t - T_d)P_H e^{-(t-T_r)/T_7}, & t > T_d \end{cases}$$

where P_0 is the intercept of the peak MAV, P_L is the amplitude of the exponential decay, P_M is the amplitude of the exponential increase, t is time measured since the beginning of the experiment (min). T_5 and T_6 are exponential time-constants (min), T_r is the time of the first recovery measurement (120 min), $(t - T_d)P_H e^{-(t-T_r)/T_7}$ is the hyperexcitability term. This term has a delayed onset during the recovery period and is equal to zero when $t < T_d$.

2.6.5. Median Frequency of the EMG

The model for the time course of the MF data was described by the equations below:

$$\mathrm{MF}(t) = \begin{cases} F_0 + F_L e^{-(t-T_r)/T_8} + F_M(1 - e^{-(t-T_r)/T_9}), & t < T_d \\ F_0 + F_L e^{-(t-T_r)/T_8} + F_M(1 - e^{-(t-T_r)/T_9}) \\ \quad +(t - T_d)F_H e^{-(t-T_r)/T_{10}}, & t > T_d \end{cases}$$

where F_0 is the intercept of the peak MF (Hz), F_L is the amplitude of exponential decay dominating beginning of recovery period (Hz), F_M is the amplitude of exponential increase following decay in beginning of recovery period (Hz), T_r is the time of first recovery measurement (120 min), T_d is the time of onset of hyperexcitability (min), T_8 is the exponential time constant of exponential decay dominating beginning of recovery period (min), T_9 is the exponential time constant of exponential increase following decay in beginning of recovery period (min), T_{10} is the exponential time constant of hyperexcitability term dominating end of recovery period (min), $F_L e^{-(t-T_r)/T_8}$ allows for exponential decay dominating beginning of recovery period, $F_M(1 - e^{-(t-T_r)/T_9})$ allows for exponential increase following decay in beginning of recovery period, $(t - T_d)F_H e^{-(t-T_r)/T_{10}}$ Hyperexcitability term with delayed onset dominating end of recovery period (equal to zero when $t < T_d$).

Again, Marquardt–Levenberg nonlinear regression algorithms were used to generate the best fit model, optimizing for the regression coefficient.

3. Results

A typical recording of load, displacement and EMG from the three lumbar levels during the six 10 min load/rest and the 7 h recovery is shown in Fig. 1. From the displacement trace, the gradual increase in the peak displacement with time is observed during each 10 minute loading period. A partial recovery in peak displacement is evident at the end of the first 10 min rest, followed with further increase in peak displacement over the second 10 min loading. The increase and partial recovery repeat to the end of the sixth loading period, ending with a maximal peak displacement. The 7 h rest period is characterized with a gradual decrease of the peak displacement, approaching the peak amplitude of the first loading cycle by the seventh hour. The EMG traces display gradual decrease of peak amplitude throughout each 10 min loading period with superimposed spontaneous, unpredictable spasms. A substantial decrease in peak EMG is evident by the sixth loading period. During the 7 h rest period, the initial peak EMG is low and steadily increasing with each hour of rest. Large amplitude spasms are observed during the single cycle loadings as well as in the period immediately after the single cycle was terminated.

Fig. 2 provides the mean creep vs. time curves during the loading period and the 7 h recovery for cyclic peak loads of 40 N @ 0.25 Hz (left panel), 40 N @ 0.5 Hz (middle panel) and 60 N @ 0.25 Hz (right panel). It is evident that the creep at the end of the six loading periods is much higher if the frequency of the flexion-extension is increased from 0.25 Hz (left panel) to 0.5 Hz (middle panel) while the peak load remains at 40 N. Similarly, a significant increase in creep is evident if the peak load is increased from 40 N (left panel) to 60 N (right panel) while the frequency remains at 0.25 Hz. Furthermore, the residual creep-Cr, at the end of the 7 h rest, is minor

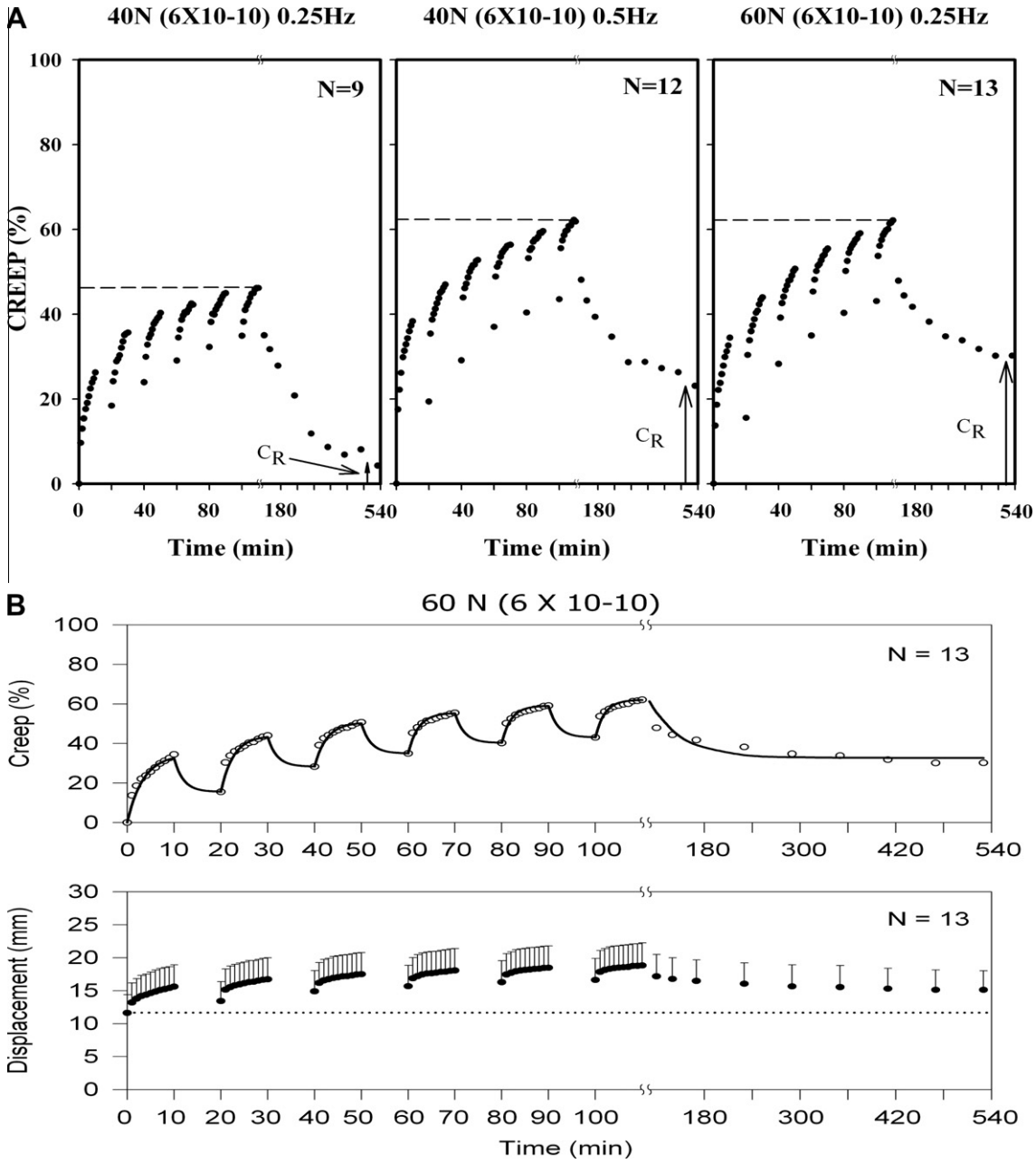

Fig. 2. (A) Mean creep vs. time for 40 N load at 0.25 Hz on the left, 40 N at 0.5 Hz in the middle and 60 N at 0.25 Hz on the right. Note the substantially larger peak creep at the end of loading and the larger Cr-residual creep associated with increased frequency and increased load. (B) A typical model of the creep fitted to the experimental data from a group of felines subjected to 60 N load applied six times for a 10 min duration/10 min rest.

for the 40 N @ 0.25 Hz (left panel) but substantially larger if the frequency (middle panel) or peak load (right panel) are increased. Higher movement velocity and higher loads, therefore, have an adverse effect on the creep, increasing its peak value at the end of loading and the residual value after 7 h of rest.

Fig. 3, left column, displays a typical mean NIEMG and displacement during a three 10 min loading session and the 7 h recovery period. Similarly, the right column displays the mean NIEMG and displacement during a nine 10 min loading session. The most prominent feature depicts a gradual decrease of the mean NIEMG during loading. During the recovery period, the mean NIEMG displays a minor transient increase at the beginning with a further gradual increase toward its baseline level observed at the initiation of the three 10 min loading session (left column) or substantially above that baseline level in the right column.

Fig. 4(A–D) display the NIEMG during the 7 h recovery period for increased load (left panel), increased number of repetitions (second from left panel), decreased rest periods between the 10 min loading periods (second from right) and increased loading frequency (right panel). The statistical analysis reveals a significant ($p < 0.0001$ to <0.01) effect of time for all the mean NIEMG data during the 7 h rest. There was also a significant ($p < 0.0001$) effect of load, significant effect ($p < 0.001$) of repetitions, significant ($p < 0.003$) effect of rest periods and significant ($p < 0.024$) effect of frequency. There was a lack of interaction between time and the variable of interest (peak load, rest period, repetitions and frequency). The common observation, therefore, is that increasing the load, the number of repetitions, decreasing the rest period and increasing the frequency of loading result in significant increase of the NIEMG over the baseline level, or muscular hyperexcitabilty

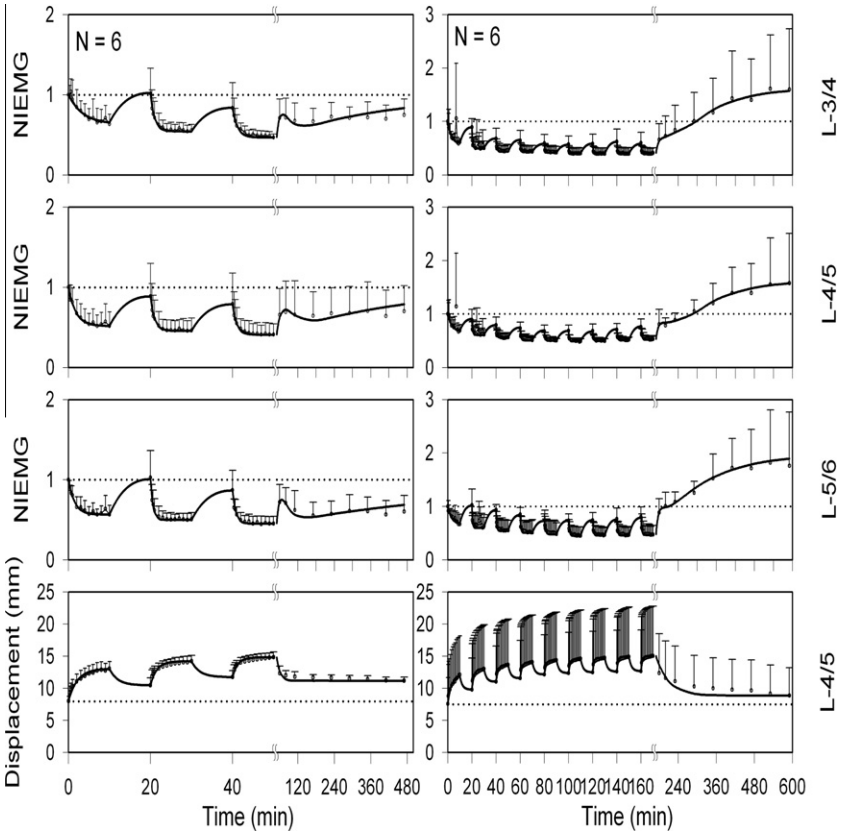

Fig. 3. Comparison of the NIEMG response during the 7 h rest for a protocol including three load/rest vs. nine load/rest sessions. The mean NIEMG during the three 10 min loading session and during the 7 h recovery is given on the left column. The mean NIEMG during a nine 10 min loading session and during 7 h recovery is given on the right column. Note the large increase in NIEMG in the right column past the first 2 h of rest, exhibiting 150–200% increase over baseline, demonstrating the hyper-excitability.

during the last several hours of the 7 h recovery period. On the other hand, low loads, low number of repetitions, low frequency and long rest periods result in a NIEMG curve that asymptotically reaches the baseline near the seventh hour of rest post-loading.

Fig. 5 displays the results of the cytokines analysis comparing their expression level at the end of the 7 h rest at low loads vs. high loads and relative to the un-stimulated self control of L_{10-11}. Significant differences ($p < 0.001$ to <0.028) exist from the expression level of the controls to that of the 20 and 60 N indicating that significant pro-inflammatory degradation of the ligaments occurred once any load was applied in a cyclic manner for a cumulative 60 min. Furthermore, significant ($p < 0.001$ to 0.019) differences exist in the expression level of IL-6, IL-8 and TGFβ, confirming that higher loads trigger higher expression level of these three cytokines. Furthermore, there was an effect of vertebral level, with L_{3-4} being marginally significant in some cases whereas L_{4-5} and L_{5-6} being significant.

Fig. 6 displays the pro-inflammatory cytokines expression at the end of the seven hours rest for the two groups loaded with the same load of 40 N but at two different frequencies. IL-6, IL-8 and TNF-α expression were significantly increased in the group subjected to the 0.5 Hz loading frequency relative to the 0.25 Hz for the three vertebral levels. Significant increase in IL-1β expression was also present for L_{4-5} and L_{5-6} as well as for TGF-β expression for L_{5-6} in the higher loading frequency group. Three of the cytokines (IL-1β, IL-8 and TGF-β) demonstrated significant interactions between loading rate and vertebral level. Post hoc analyses revealed that L_{4-5} expression levels were greater than L_{3-4} expression levels in each of these cytokines. IL-6 and TNF-α had significant main effects of loading frequency ($p = 0.020$ and 0.037, respectively) in which cytokines expression were significantly larger in the higher frequency group. Vertebral level also demonstrated a significant effect ($p = 0.001$) in IL-6 in which L_{4-5} expression levels were larger then L_{3-4} levels. This indicates that tissue degradation is significantly more severe with exposure to higher movement velocity.

Fig. 7 provides the definitions of the DNNZ and TNNZ superimposed on a typical single cycle of load, displacement and EMG recorded from one preparation.

Fig. 8 displays the mean ± SD of the DNNZ for each loading condition (20 N on the upper row and 60 N on the lower row) before and after cyclic loading. For the 20 N loading condition, each of the lumbar levels demonstrated an increase immediately following the cyclic loading period and then gradually decreased toward baseline values. Statistical analyses revealed no phase × time interactions for the L_{3-4} and L_{4-5} levels ($p = 0.360$ and 0.769) along with significant main effects of time ($p < 0.001$ for each level) and a significant interaction for the L_{5-6} level ($p = 0.048$). The interaction in L_{5-6} occurred because the DNNZs during the stretch phase did not return to baseline while the relaxation phase did during the last hour of the recovery period. Baseline values for the stretch phase were 2.7, 2.0, and 2.1 mm for the L_{3-4}, L_{4-5} and L_{5-6} levels, respectively. These values had increased approximately 2.4–3.3 times when measured immediately after the cyclic loading. Baseline relaxation values were 4.3, 4.7 and 4.6 mm, respectively, and increased approximately 2.0–2.2 times when measured after the cyclic loading. During the recovery period DNNZs decreased to 3.5, 3.3 and 3.6 mm (stretch phase), respectively, and 5.9, 5.7 and 5.4 mm (relaxation phase), respectively, by the end of the recovery period. The 60 N loading condition also demonstrated an increase

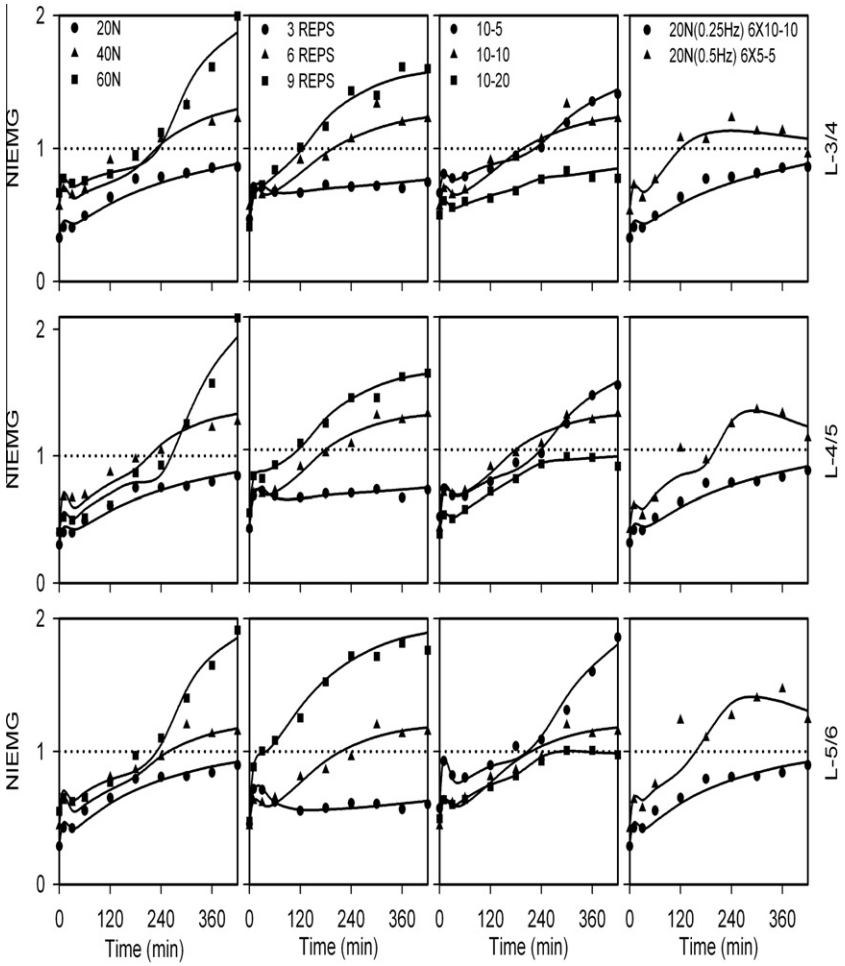

Fig. 4. Mean NIEMG vs. time during the 7 h recovery period for increasing load (left), increasing number of repetitions (second from left), decreasing duration of rest in between the 10 min loading periods (second from right) and for increasing frequency (right).

measured immediately after the cyclic loading period followed by a gradual decrease toward baseline values. There were no phase × time interactions for any of the lumbar levels ($p = 0.605$, 0.632, and 0.619), and all three levels demonstrated a significant main effect of time ($p < 0.001$ for all levels). The mean baseline values for the stretch phase were 6.1, 6.0, and 5.6 mm for the L_{3-4}, L_{4-5}, and L_{5-6} levels. These values had increased approximately 2.2–2.3 times when measured immediately after the cyclic loading period. The mean baseline relaxation values were 9.9, 9.7 and 9.8 mm, respectively, and increased approximately 1.7–1.8 times above baseline when measured after cyclic loading. The DNNZs remained significantly elevated more than 4 h following cyclic loading at the L_{3-4} and L_{4-5} lumbar levels, and more than 5 h at the L_{5-6} lumbar level. By the end of the recovery period the mean DNNZs had decreased to 5.9, 6.1, and 5.3 mm (stretch phase) and 11.1, 11.2, and 12.2 mm (relaxation phase) and were not significantly different from the baseline.

Fig. 9 displays the mean ± SD of the TNNZ for each loading condition (20 N on the upper row and 60 N on the lower row) before and after cyclic loading. In the 20 N loading condition, there were no phase × time interactions for any of the L_{3-4} and L_{4-5} lumbar levels ($p = 0.390$ and 0.881). These levels demonstrated significant main effects of phase ($p < 0.001$ for each level) and time ($p < 0.001$ for each level). A significant phase × time interaction ($p = 0.030$) was found in the L_{5-6} level since the TNNZ for the stretch phase did not change significantly following the cyclic loading period while the TNNZs measured during the relaxation phase demonstrated a similar significant change pattern as the L_{3-4} and L_{4-5} levels. The baseline values for the stretch phase were 5.0, 3.8 and 4.1 N for the L_{3-4}, L_{4-5} and L_{5-6} levels, respectively. These values increased approximately 1.6 and 1.9 times above baseline within 30 min following the cyclic loading period in the L_{3-4} and L_{4-5} lumbar levels only. The baseline relaxation values were 9.7, 8.7 and 7.9 N, respectively, and increased approximately 1.4–1.5 times above baseline within 30 min following the cyclic loading period. The TNNZs remained significantly elevated through 1, 2, and 2 h during the recovery period for each of the lumbar levels, respectively. Afterward, the TNNZ values decreased below baseline, although not statistically significant to 3.9, 3.8, and 4.7 N (stretch phase) and 7.8, 6.8, and 5.5 N (relaxation phase) by the end of the recovery period. There were no phase x time interactions in the 60 N loading condition for any of the lumbar levels ($p = 0.792$, 0.889, and 0.791), but demonstrated significant main effects of time ($p < 0.001$ for all levels). The baseline values for the stretch phase were 21.3, 20.3 and 18.9 N for the three levels, respectively. The baseline values for the relaxation phase were 37.2, 33.3 and 35.7 N for L_{3-4}, L_{4-5} and L_{5-6} levels, respectively. Each lumbar level demonstrated significant increases of 1.5, 1.4, and 1.3 times (stretch) and 1.2, 1.2, and 1.3 times (relaxation) above baseline values within 10 min following the cyclic loading period. The TNNZs remained significantly elevated for 1 h in $L_{3/4}$ and for 2 h in $L_{5/6}$, but decreased back to baseline by the end of the first hour in $L_{4/5}$. The TNNZs for each lumbar level significantly decreased below baseline by the fifth hour of the recovery period

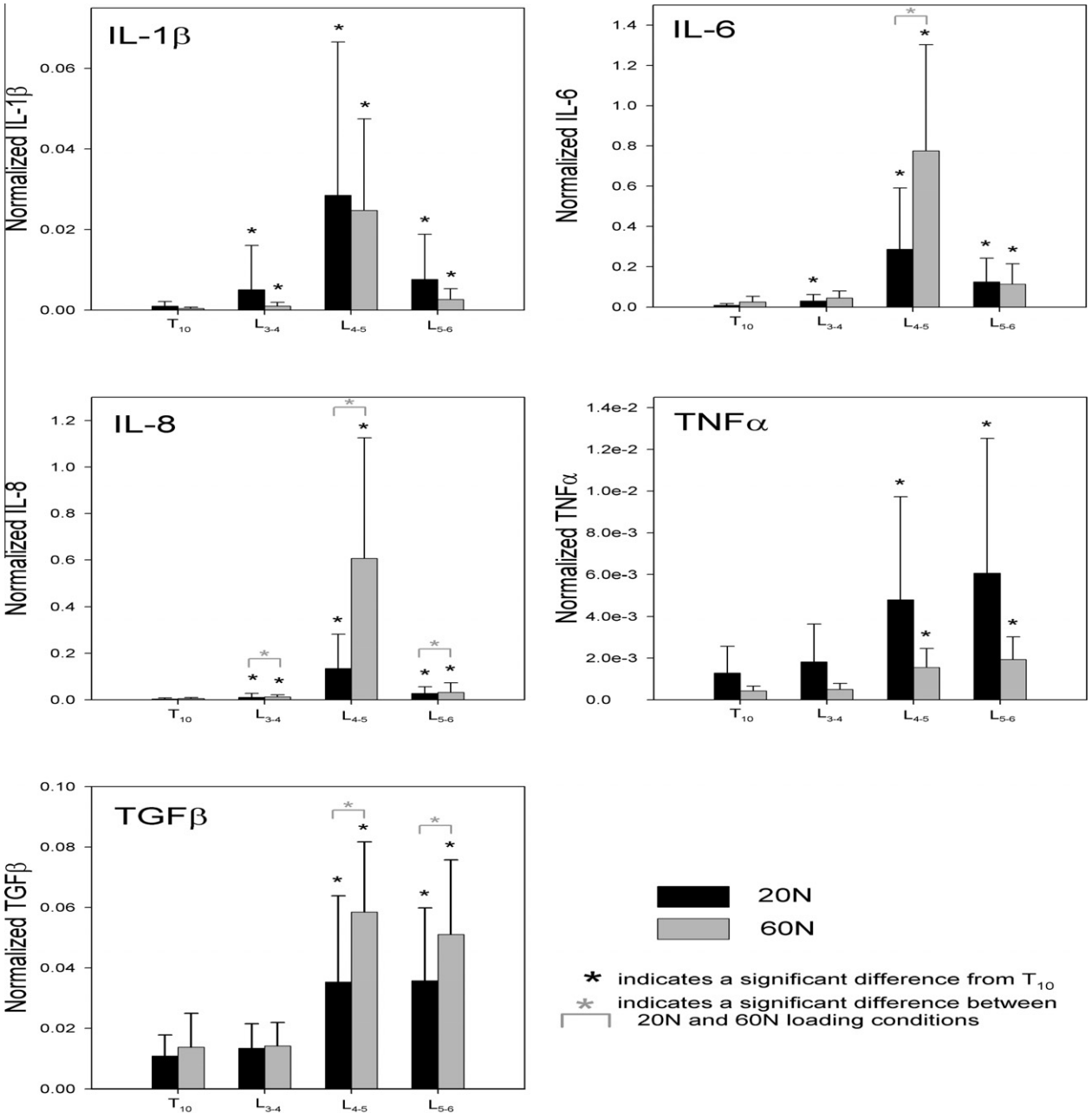

Fig. 5. Cytokines expression level of the group loaded with 20 N relative to the group loaded with 60 N and compared to the self control L_{10-11}.

to final values of 7.6, 9.2 and 5.2 N (stretch phase) and 20.5, 22.8 and 28.8 N (relaxation phase) for the three levels, respectively.

For each lumbar level, both the DNNZs and TNNZs measured during the stretch phase of loading were significantly smaller than those measured during the relaxation phase of loading ($p < 0.001$ for all levels). The differences between the loading phases have been discussed in detail in a previous publication.

Fig. 10 displays the mean ± SD of the PMAV for each loading condition (20 N on the upper row and 60 N on the lower row), before and after the cyclic loading period. In the 20 N loading condition, significant changes with time were found in L_{3-4} ($p = 0.004$) and L_{4-5} ($p = 0.040$) levels while L_{5-6} did not vary significantly with time ($p = 0.114$). Pair wise comparisons revealed a significant decrease to 68% and 69% of the baseline values within the first hour of recovery for the L_{3-4} and L_{4-5} levels, respectively. Following this decrease, there was a gradual, but insignificant, increase in the mean values to baseline and further above, although not statistically significant.

In the 60 N loading condition, significant decreases to below baseline were found at each lumbar level ($p < 0.001$ for all levels) when measured immediately after the cyclic loading period. These values decreased to 64%, 66%, and 66% of baseline within the first hour and returned to baseline before the third hour of the recovery period. A further increase above baseline by the third hour of the recovery period was also present, although not statistically significant.

Fig. 11 displays the mean ± SD of the MF for each loading condition (20 N on the top row and 60 N on the bottom row) before and after cyclic work. In the 20 N loading condition, significant changes with time were found at the L_{4-5} level ($p = 0.008$) while no changes were found with time at the L_{3-4} ($p = 0.268$) and L_{5-6} ($p = 0.150$) levels. Pair wise comparisons revealed a 10% decrease in MF at the L_{4-5} level measured after the cyclic loading period and a

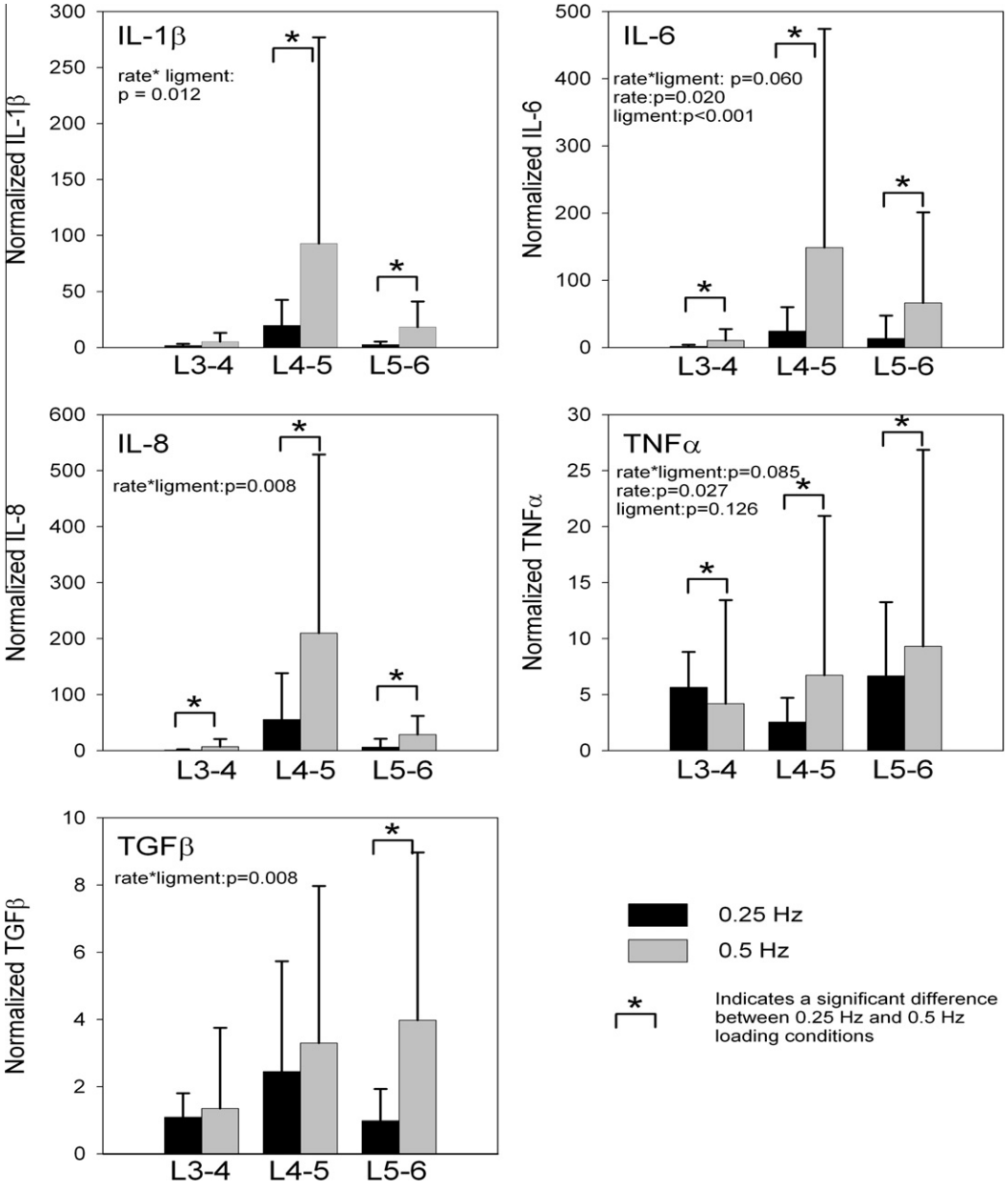

Fig. 6. Cytokines expression level of the group loaded with 40 N peak load at frequency of 0.25 Hz and the group loaded with 40 N at a frequency of 0.5 Hz.

gradual increase to baseline by the fourth hour of the recovery period. For the 60 N load, L_{4-5} and L_{5-6} demonstrated significant changes with time ($p = 0.025$ and 0.001) while L_{3-4} did not change ($p = 0.123$). The MF significantly decreased in L_{5-6} within 30 min following cyclic work and gradually increased to the baseline after the first hour of the recovery period. Both L_{4-5} and L_{5-6} demonstrated a significant increase in MF at the sixth and seventh hours during the recovery period.

The best fit models designed for each of the parameters discussed above are superimposed on the mean ± SD data presented in the corresponding figures. In general, the fit quality was high, with $r^2 \geqslant 0.87$. In the NIEMG data during the cyclic loading period, the quality of the fit was occasionally lower due to the random and unpredictable spasms superimposed on the EMG which were present in the conditions of high loads, high frequency of loading and many repetitions.

4. Discussion

The primary finding emerging from the experimental data consists of scientific, experimental evidence identifying the lumbar viscoelastic tissues as the organ that fails when exposed to prolonged repetitive loading and inflammation as the mode of failure. Furthermore, the cumulative disorder defined by the complex interaction of the viscoelastic tissues biological and mechanical properties with the motor control and stability of the lumbar spine during the repetitive loading and during the following acute inflammation phases were identified and modeled. Finally, experimental evidence were provided to support the epidemiology in designating specific severe loading conditions as high risk for the development of cumulative disorder. Overall, a broad, multifactorial and interactive insight into the various components active in the development of a cumulative disorder was obtained.

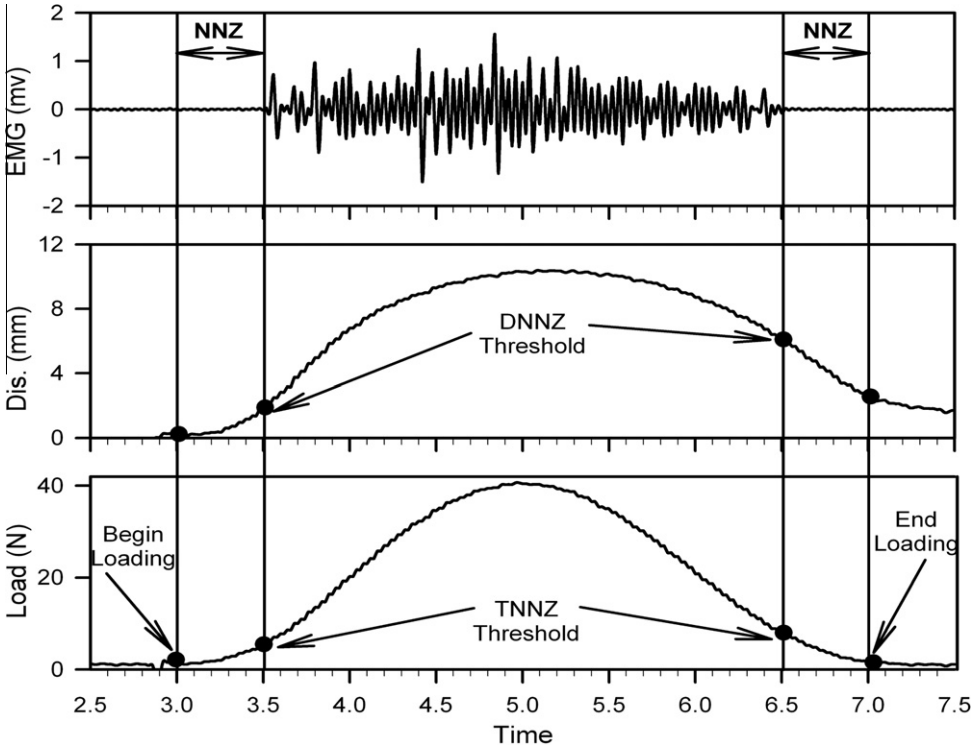

Fig. 7. Typical recordings of a single cycle flexion-extension with a peak load of 40 N (bottom trace). The associated displacement (middle trace) and the EMG (top trace) as well as the marked definitions of DNNZ and TNNZ are delineated. Increasing DNNZ and TNNZ indicate decrease in stability as the muscles are active for shorter segments of the flexion-extension.

A common finding throughout the results is the presence of spasms during the loading period. This was observed regardless of the load magnitude, frequency of loading, number of repetitions, etc. The spasms occurred randomly, in an unpredictable manner and were present more often under high loads and high frequency loading. From the neurological standpoint, they represented injury potentials triggered by the occurrence of the micro-ruptures in the collagen fibers of the strained viscoelastic tissues. Indeed, the results of the cytokines analysis indicates that significant increase in expression was observed in the supraspinous ligaments subjected to low, as well a as high magnitude loads. The increase in the pro-inflammatory cytokines supports that micro-ruptures may have occurred in both loading conditions. Since the expression level was significantly higher in the ligaments subjected to high risk loads relative to ligaments exposed to low risk loads, one can infer that the tissue degradation (or micro-damage) was larger under high loads and high frequencies. This fully justify the designation of high magnitude loads, multiple repetitions, short in between rest periods and high frequency loading as "high risk". One can also assert, however, that a condition of "no risk" is probably non-existent. A "low risk" may be a better description, since increase in pro-inflammatory cytokines is present and indicates tissue degradation as well as deficient stability for several hours post loading.

Another common finding throughout the results is the significant increase in the NIEMG during the last few hours of the 7 h rest period post-loading when the loads were high, at high frequency, repeated many times or with a short in-between rest. The increase in the NIEMG ranged from 10% to 15% over the baseline for moderate loading conditions to over 100% increase for extreme loading conditions. This feature was repeatable reliably and could predict that the loading condition was at high risk of an acute inflammation. The cytokines data together with the sharp increase in neutrophil density in the tissue we presented earlier (Solomonow et al., 2003) confirm this observation by demonstrating the highest expression levels in cases where the NIEMG in the last 2–3 h of the rest periods was the highest.

Did the increase in cytokines expression level in the viscoelastic tissues trigger the increase in the NIEMG? Most likely so. Inflammatory conditions in neurological/viscoelastic tissues are known to trigger neuromuscular hyperexcitability (Bove et al., 2003; Dilley and Bove, 2008; Cavanaugh et al., 2006). The hyperexcitability in the muscles nearby the inflamed/damaged tissue increases the stiffness of the joint, limit the range of motion and prevent or minimize additional strain and exposure to further injury.

Conversely, loading conditions consisting of light loads, low frequency with low repetitions and long in-between rest did not exhibit the muscular hyperexcitability in the last few hours of the 7 h post-loading rest. The NIEMG exhibits a gradual slow recovery to baseline. Again, while the NIEMG does not imply a high risk of excessive micro-damage due to the loads applied, the expression level of several pro-inflammatory cytokines does increase significantly over baseline, indicating some tissue degradation. Perhaps there is a threshold level of damage which triggers an acute inflammation and muscular hyperexcitability and that should be investigated in the future. Another possibility is the presence of the pain mediator cytokine, IL-8. It was shown that IL-8 has a role in pain initiation (Wang et al., 2009). The expression level of IL-8 in the light load group was low and perhaps below the level necessary to trigger pain. Alternatively, it could be the pain component associated with IL-8 that triggers the muscular hyperexcitability. Evidently, additional research into this issue is in order. Nevertheless, within the physiological load range (Solomonow et al., 1998) tested in these series of studies, elevated cytokines expression together with spasms/injury potentials during the loading period lead one to assume that a low risk and high risk loading conditions exist for the triggering of an acute inflammation, excluding a no risk category.

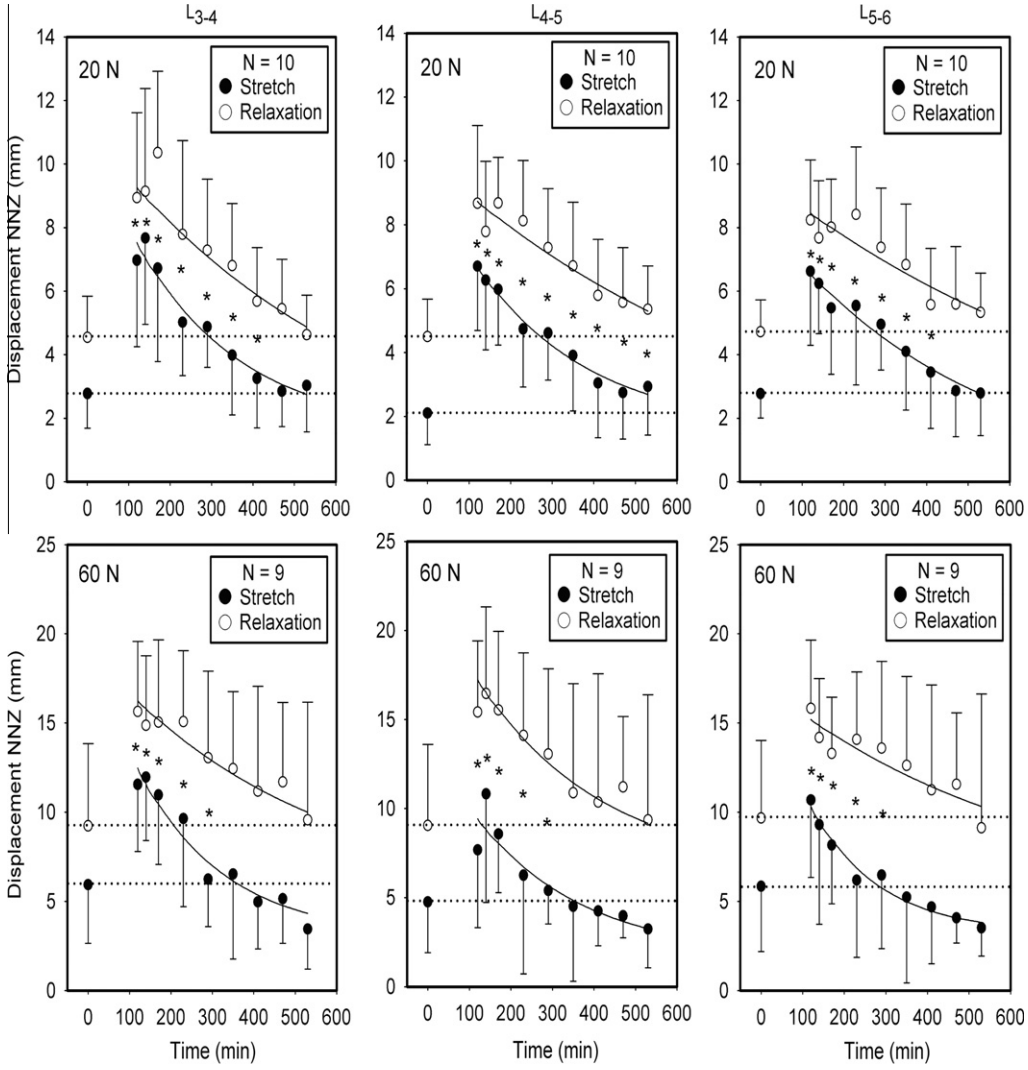

Fig. 8. The DNNZ for flexion and extension of the three lumbar levels during the 7 h rest period post loading with a peak of 20 N (top trace) and with a peak load of 60 N (bottom trace).

High loads, many repetitions, short rest and high loading velocity (frequency) are, therefore, categorized by the data emerging from this research as "high risk" for the development of cumulative disorder and confirm the epidemiology. High loading frequency deserves special attention. When comparing 20 and 60 N loads applied at 0.25 Hz, we were able to show in the 60 N data, many spasms during loading and muscular hyperexcitability with superimposed spasms during the last 4 h of the 7 h of post-loading rest. Furthermore, we also observed significantly increased cytokines expression level and significant motor control compensation of compromised stability (or hyper-stability/stiffness) within an hour post-loading. With such observations it was concluded that a 60 N load, a high but physiological load, is a risk factor for cumulative disorder development. From another perspective, 20 N peak load applied within 2 s corresponds to a 10 N/s loading rate. Conversely, 60 N peak load applied within 2 s, however, corresponds to a loading rate of 30 N/s. In such a loading paradigm, we did not compare only a peak load of 20 N to a peak load of 60 N, but also loading rates of 10–30 N/sec. Viscoelastic tissues functional properties and integrity is heavily dependent on loading rate (or strain rate). High strain rates are known to cause development of high tensions within the tissues and lower the failure load (Panjabi and Courtney, 2001; Solomonow, 2004). It is obvious that substantially larger micro-damage could be present in the tissues of the 60 N group due to the increased loading rate in addition to the higher load. This may have contributed to the increase in cytokines expression, muscular hyperexcitability, motor control compensation of compromised stability and large residual creep. It emerges that high frequency or more precisely, high loading rate is perhaps the most prominent risk factor, having direct impact on tissue damage, the resulting degradation/inflammation and the associated changes in motor control, stability and residual creep.

The motor control component is important as it has implications on spine stability, posture, performance and exposure to injury. Muscular activity emerges from motor centers for task executions as well as reflexively from afferents in the ligament, discs, and facet capsule (Solomonow et al., 1998; Stubbs et al., 1998; Indahl et al., 1995; Cavanaugh et al., 2006; Azar et al., 2009, Pickar, 1999; McLain and Pickar, 1998). Recently, the muscle spindles in the multifidi were shown to be extra sensitive to vertebrae motion relative to other paraspinal muscles and probably have a prominent role in reflexive activation (Cao et al., 2009). The reflexive activity of the multifidi muscles recorded in this project demonstrate several patterns which strongly interact with the creep/laxity of the viscoelastic tissues as well as with their pro-inflammatory status. During the loading periods, the NIEMG exhibits gradual, exponential decrease. This

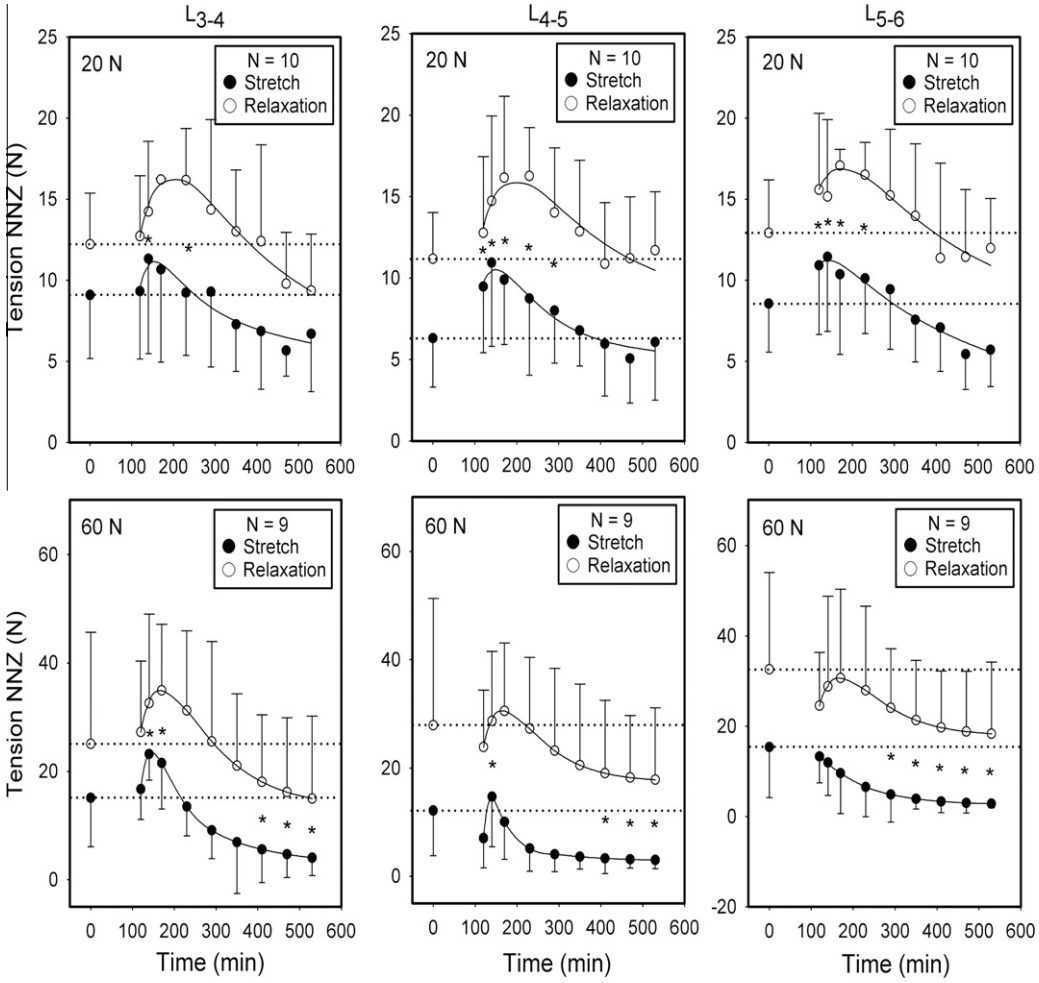

Fig. 9. The TNNZ for flexion and extension of the three lumbar levels during the 7 h rest post loading with a peak of 20 N (top trace) and 60 N (bottom trace).

decrease is concurrent with the exponential rise in creep recorded from the viscoelastic tissues. Since the viscoelastic tissues develop gradual increase in laxity with loading, their baseline tensions decrease and the trigger threshold of afferents gradually shifts such that less motor units are activated as loading time increases. In essence, the two major components responsible for spine stability are gradually becoming less functional with time; e.g. increased laxity of the viscoelastic tissues in parallel with decreasing muscular activity. Indeed, the TNNZ and DNNZ show significant increase immediately after loading. This period, therefore, is the most vulnerable to potential injury even from simple unloaded motion. Fortunately, motor control compensation kicks in within an hour, stiffening the joint to levels above normal.

In cases when the loading conditions were light (light load, few repetitions, slow motion, etc.) the tension and displacement NNZs demonstrate several hours of deficient function, as they are larger than normal and decrease slowly towards baseline. Eventually, 5–7 h of rest allow return to near baseline together with the reduction of viscoelastic laxity to near baseline. Nevertheless, at least 5 h of decreased stability is present and requires caution in order to prevent injury. This adds a new and important dimension to the "low risk" designation assigned to low loads, few repetitions, etc. discussed above. The earlier designation was based only on tissue degradation due to moderate increase in cytokines expression and now a prolonged deficit in stability is added, further asserting that the "no risk" category is non-existent.

Under loading condition designated as high risk, the decrease in muscular activity as expressed by reduction in the MF (or active motor units) as well as peak EMG is also observed in the first hour post-loading. Since this is also in parallel with laxity in the viscoelastic tissues, the overall stability of the spine is deficient and exposure to injury is present. In this case, however, a swift compensatory motor control mechanism comes into play and triggers a significant increase in muscular activity. This hyper-excitability ranges from 20% to 200% increase over baseline muscular activity which induces substantial increase in stiffness and shielding from possible injury. The compensation is for the severe laxity in the viscoelastic tissues which require many hours to be restored. Furthermore, since the amount of micro-damage in the collagen fibers is probably large, a deficit in baseline viscoelastic tension is expected until the acute inflammation is terminated with their healing. Indeed, the residual creep under high risk conditions is large and asymptotic, indicating that a new physiological process needs to kick in before the creep is fully restored (D'Ambrosia et al., 2010). The muscular hyper-excitability, therefore, is compensating for the long-term reduction in viscoelastic tissues function. It also shields the damaged tissue from further injury. The triggering source of the hyper-excitability is probably the inflammatory status of the viscoelastic tissues (Cavanaugh et al., 2006, Bove et al., 2003; Dilley and Bove, 2008) or the associated pain with the IL-8 high expression level. Two sources of autonomic motor activation of the musculature exist; the reflexive actuation from afferent

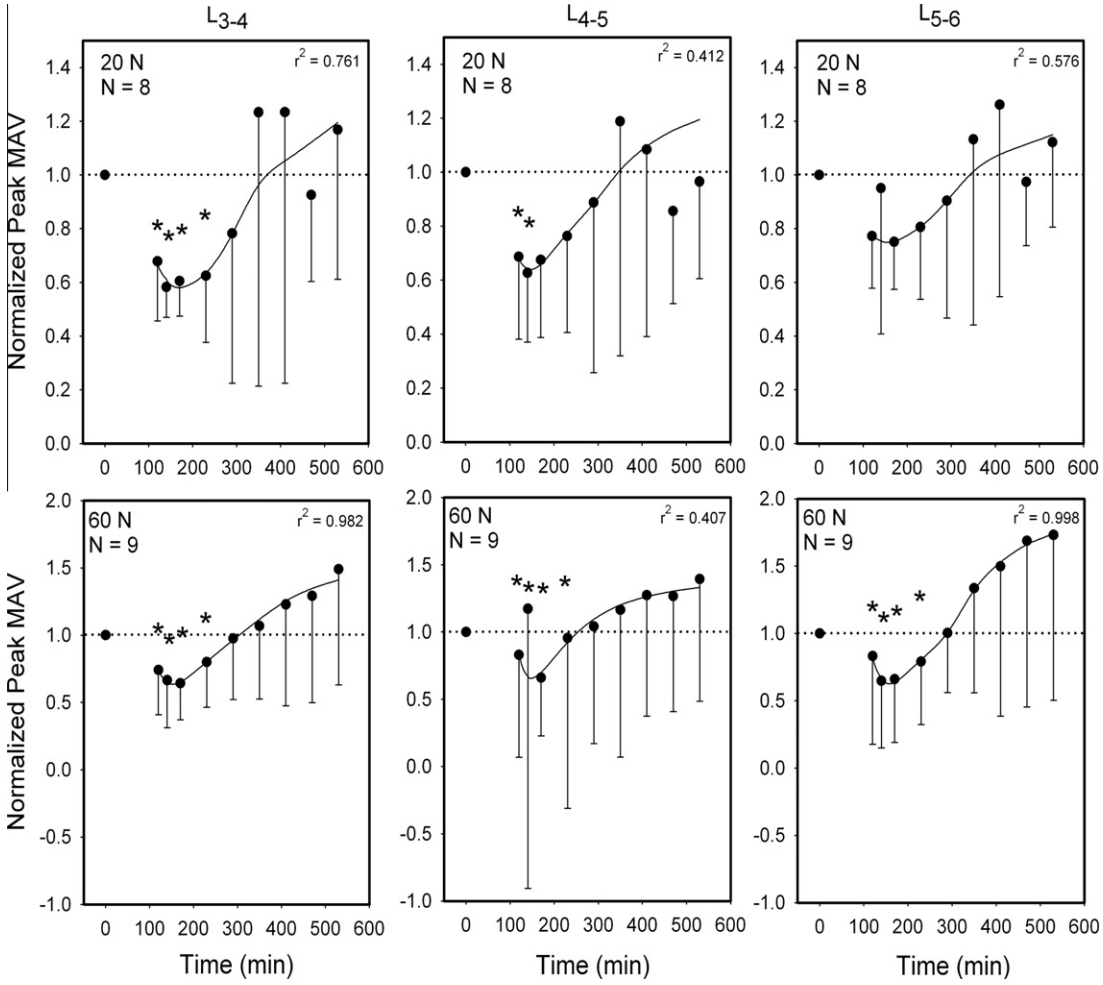

Fig. 10. The Peak MAV of the EMG as a function of time during the 7 h rest period post loading at peak of 20 N (top trace) and 60 N (bottom trace).

and the pro-inflammatory status of the same viscoelastic tissues. Since the viscoelastic tissues are still lax, their inflammatory condition is most likely the source of the motor control compensation.

In order to optimize the gained information and obtain a comprehensive overview of the lumbar cumulative disorder, the various components, including the creep, muscular activity, stability and pro-inflammatory cytokines expression could be presented on a common time axis. Providing such a common time base further increases our ability to observe and understand the sequence of events and interaction between the components. Fig. 12 provides a schematic presentation of the creep, muscular activity, cytokines expression and stability during the loading period and the following hours of rest for low risk loading conditions whereas Fig. 13 provides a similar schematic presentation for high risk loading conditions (high loads, many repetitions, high frequency, etc.). Alternatively, Fig. 14 provides a flow chart depicting the various components active in the development of a cumulative disorder and the shifting interaction between them from the acute to the chronic phase.

In Figs. 12 and 13, the creep trace is used as the driving factor for understanding the multi component syndrome. In Fig. 12, the gradual increase in creep (bottom) to the end of the loading period represents the laxity developed in the functional collagen fibers (due to the strain imposed by the flexion) as well as from the non-functional fibers in which micro-damage occurred. Simultaneously, the reflexive EMG decreases (top) due to the shifting tension/strain threshold of the afferents in the viscoelastic tissues. Spasms are superimposed on the decreasing EMG, representing the injury potentials triggered by micro-damage to some collagen fibers. In turn, the stability, as expressed by the displacement and tension neutral zones decreases gradually. This is, in effect, the combined impact of increased laxity in the viscoelastic tissues and the decreased EMG amplitude and shifting initiation/termination timing of the muscular activity. The baseline level of neutrophils density in the ligaments at the initiation and termination of the loading period is unchanged, indicating that the inflammation was not initiated during the loading.

During the post-loading rest period, the creep gradually recovers, reaching near baseline level by the seventh hour. Since we identified low-risk loading activity as having minor tissue micro-damage/degradation as defined by increase in neutrophiles and pro-inflammatory cytokines expression (D'Ambrosia et al., 2010), the model accounts for a minor micro-damage in the viscoelastic collagen fibers which prevents the full recovery of the creep without undergoing the repair phase of inflammation. Typically, low-risk loading paradigms result in a residual creep value of 5% at the seventh hour. Simultaneously, the EMG displays a short spike (which is common in the first few minutes following a period of prolonged muscular activation) then gradually increases to baseline level near the seventh hour of rest. The increase in EMG is driven by the recovery of the creep and the gradual return of the excitation tension/strain threshold of afferents in the viscoelastic tissues to their baseline level and restoration of the reflexive activation of the musculature. With the recovery of creep and

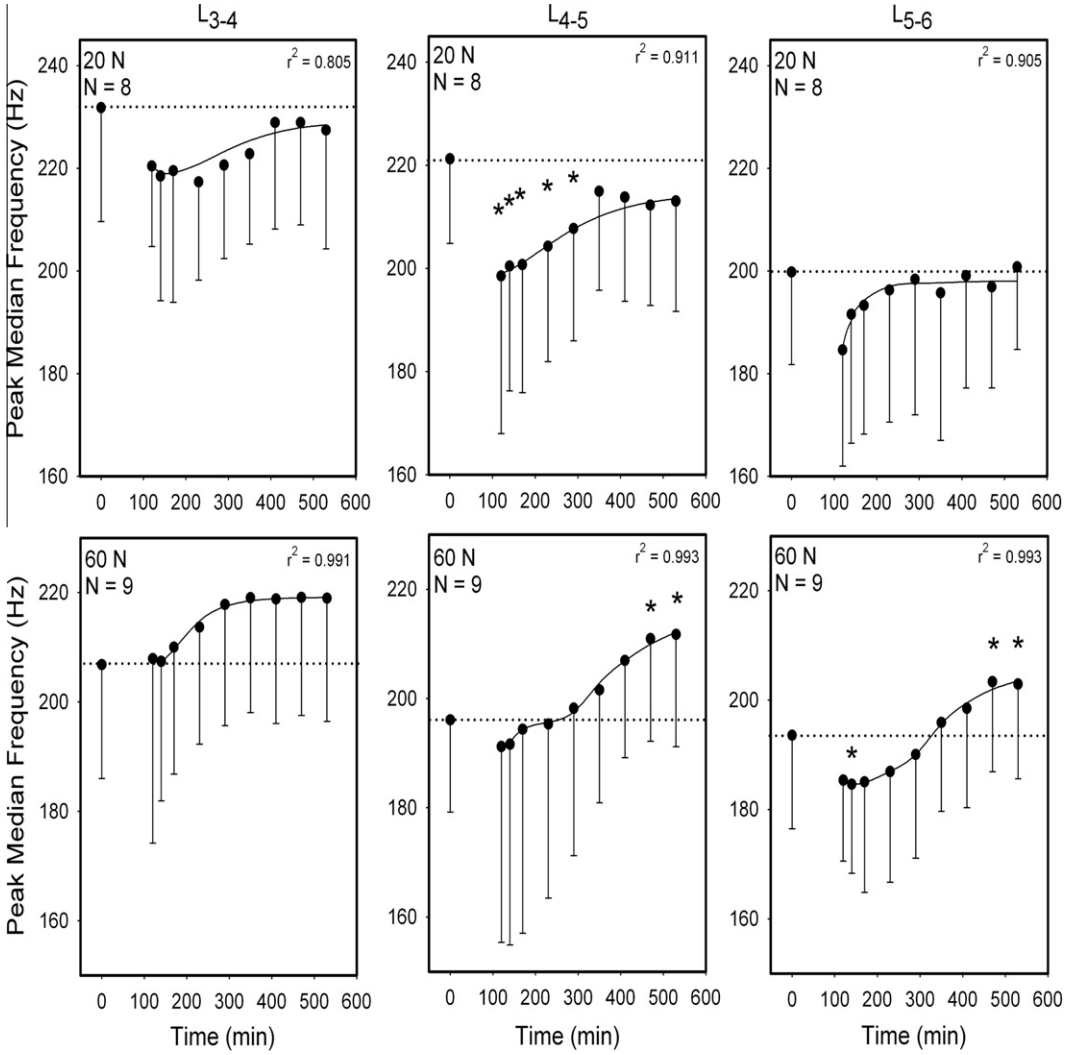

Fig. 11. The MF of the peak EMG during the 7 h post loading rest. The MF for peak load of 20 N is shown on the top trace and for a peak load of 60 N on the bottom trace.

muscular activity, the Neuromuscular Neutral Zones are also restored to near baseline by the seventh hour of rest. Nevertheless, 5–6 hours of deficient stability post-rest is present, during which risk of injury is high. Pro-inflammatory cytokines and neutrophil levels show a minor increase, pointing out the presence of some tissue damage/degradation which may be sub-clinical but in need of repair.

The comprehensive view provided in Fig. 13 for high-risk loading conditions also describes a gradual decrease in EMG with superimposed spasms during the loading period. Similarly, the creep increases simultaneously and the overall impact of the decreasing muscular activity and increasing laxity in the viscoelastic tissues results in decreased stability. Neutrophil and cytokines level are at baseline during loading.

During the post-loading rest period, the creep displays a simultaneous decrease towards baseline, but with a large residual at the seventh hour. Commonly, this residual value was near 25–30% of baseline, representing the non-functional collagen fibers affected by micro-damage. As hypothesized in our previous paper (D'Ambrosia et al., 2010), the damaged fibers will be restored back into function once the second phase of inflammation is completed with the repair of the micro-damage (Leadbetter, 1990). The repair and full restoration to function is depicted by the second exponential decrease in the creep trace, bringing it to baseline. Simultaneously, the EMG displays the small post-work spike and then a fast increase to well above baseline within the third to fourth hour post-loading. This increase, commonly in the 25–100% of baseline, is a motor control response to the inflammation/pain developing in the viscoelastic tissues. Indeed, the neutrophil and pro-inflammatory cytokines expression level displays a significant increase at the seventh hour of rest. The stability trace depicts the deficiency created by low muscular activity and viscoelastic laxity in the first hour followed by a sharp increase in stability, or hyperstability, triggered by the inflammation/pain and its associated muscular hyperexcitability. In essence, the motor control system is compensating for the viscoelastic laxity imposed by a prolonged acute inflammation as well as protection from further damage to the tissue. As the inflammation is gradually completed by restoring function to the viscoelastic tissues, stability, creep and hyperexcitability and muscular function return to baseline.

Again, the creep which represents the viscoelastic functional integrity is the driving factor of the Figs. 12 and 13. As the creep develops, the laxity of viscoelastic tissues decreases the reflexive muscular responses. The creep component representing the micro-damage in the collagen fibers triggers the inflammation/pain and the resulting muscular hyperexcitability. The combined effort of the creep and muscular activity level form the stability status at any given time during the loading and rest. Creep, therefore, is a fundamental issue in this cumulative syndrome.

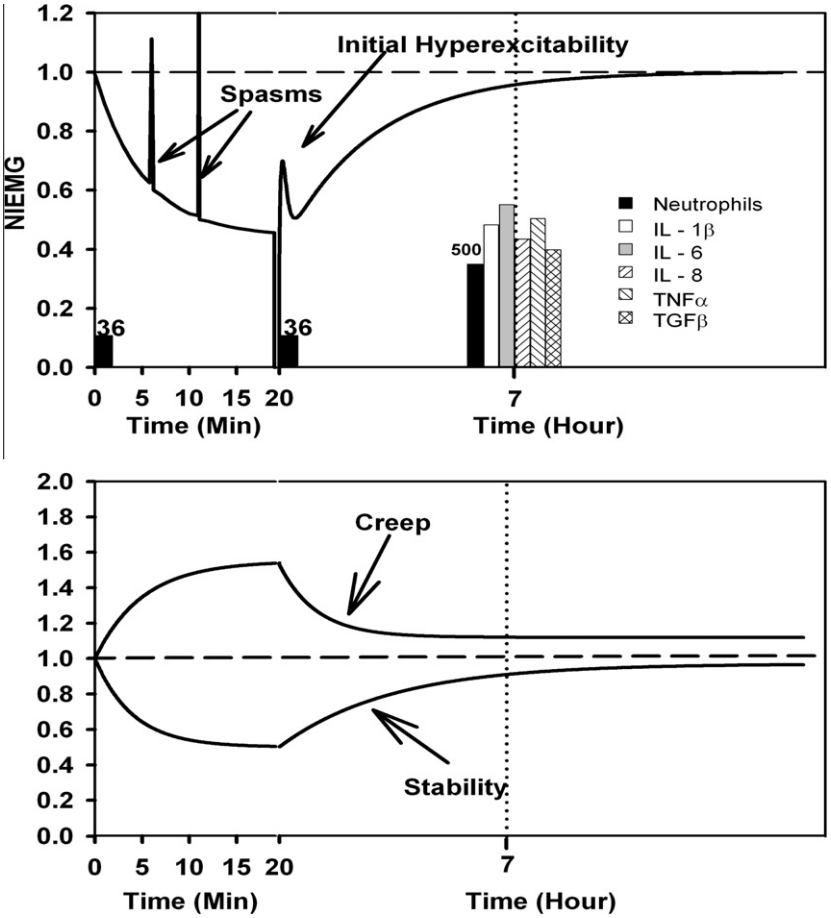

Fig. 12. A comprehensive model of; creep, neuromuscular control, tissue biology and stability during and following loading under low risk conditions.

Fig. 14 is an attempt to describe Figs. 12 and 13 in a flow chart form which is preferred by some individuals. It was also ventured to predict the development of chronic inflammation if further exposure to work is allowed in the presence of acute inflammation.

4.1. Applicability to other viscoelastic tissues

The lumbar spine was subjected to cyclic flexion-extension. This type of work strained the posterior ligaments, dorso-lumbar fascia, facet capsule and the discs. Pro-inflammatory cytokines and neutrophils analysis was limited only to the supraspinous ligament from various considerations, but one should not exclude the possibility that significant increase in pro-inflammatory cytokines and neutrophiles was present in the other posterior viscoelastic tissues. The discs, facet capsule and the dorso-lumbar fascia are tissues that behave very similarly to the supraspinous ligament and could be sites where inflammatory conditions could be triggered under cyclic load. This issue needs to be addressed with further research.

4.2. Applicability of animal data to humans

The cumulative syndrome defined in this report was demonstrated experimentally in the feline model-a quadruped. The literature provides repeated verifications that the quadruped spine is an appropriate model from biomechanical considerations (Ianuzzi et al., 2009, 2010; Smit, 2002; Wilke et al., 1997 and many others). Furthermore, the feline is a classical model in the neuromuscular/motor control literature as it closely resembles human functions such as reflexes, force-velocity and length-tension relationships in muscles, fiber type composition, motor unit recruitment, etc. (Mountcastle, 1974; Pickar, 1999). One can safely assume that the conceptual principals of operation of the cumulative trauma syndrome described in this report are identical in humans. Certainly, issues such as scaling and increased robustness of ligaments and discs in the upright human will result in larger coefficients and longer time constants relative to those obtained in the models designed for the feline.

Furthermore, recent experimental work with humans in the author's laboratory (Olson et al., 2004, 2006, 2009; Li et al., 2007) and in other laboratories around the world (Sanchez-Zuriaga et al., 2010; Little and Khalsa, 2005; Granata et al., 1999, 2005; Shin and Mirka, 2007; van Dieen et al., 2003; Kumar and Prasad, 2010; Dickey et al., 2003; Karajcarski and Wells, 2006; McGill and Brown, 1992; Hendershoot et al., 2011) confirm the development of creep, spasms, changes in EMG reflex amplitude and latency, motor control and stability following prolonged cyclic work as was described in the in-vivo feline model of this report. The increase in the neutrophil density and cytokines expression level is yet to be confirmed experimentally in humans exposed to repetitive lumbar work, as only initial confirmation is available to date (Yang et al., 2011).

4.3. Clinical and industrial implications

This report provides a comprehensive, multi-dimensional insight to the development of the *acute* phase of cumulative lumbar disorder and the prominent risk factors that trigger it. Additional research is required to experimentally demonstrate that continued exposure to the risk factors past the acute phase lead to the *chronic* phase. Based on the valuable information already available (Leadbetter, 1990), one can assume with a high level of confidence

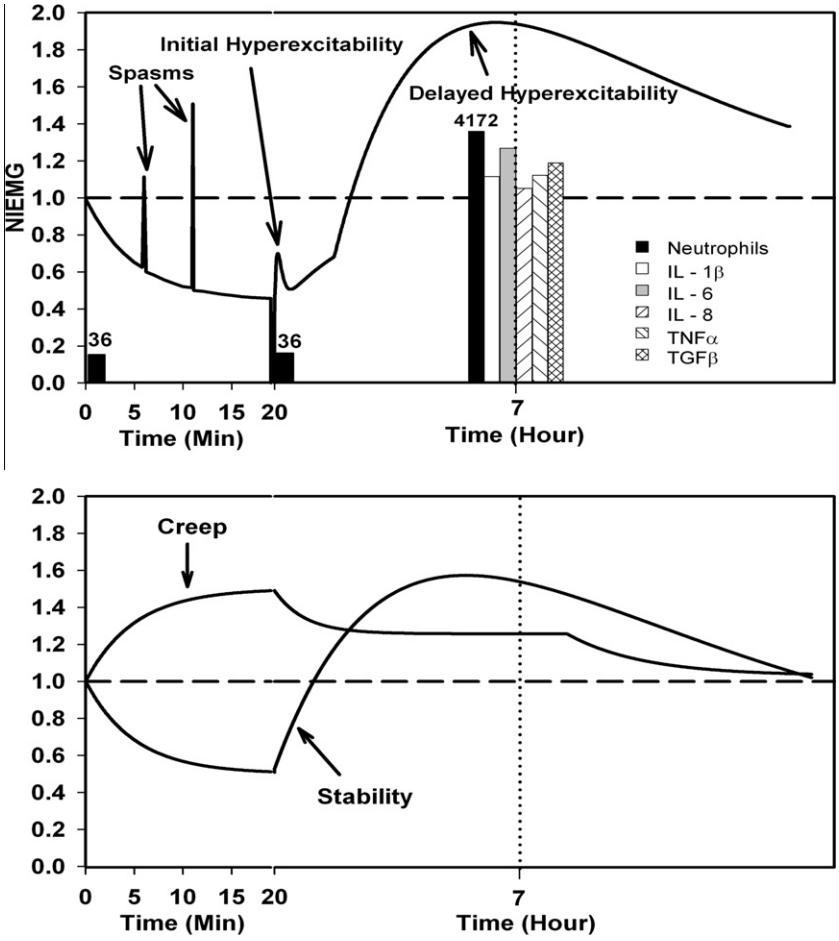

Fig. 13. A comprehensive model of; creep, neuromuscular control, tissue biology and stability during and following loading under high risk conditions.

that the chronic phase will indeed be triggered with continued exposure to cyclic work. The insight provided here on the acute phase, however, is significant and valuable for several reasons. For example, once the acute phase is diagnosed/observed in workers, various therapeutic and preventive measures could be employed to treat it and prevent it from progressing to the chronic phase. Work managers, for example, can remove such employee from activities requiring spinal loading and rotate them to duties requiring upper or lower extremity work. This will allow the rest required for spontaneous recovery of the acute lumbar inflammation or recovery while on pharmaceutical or clinical treatment.

An important clinical implication is in the diagnostic phase. Once the initial standard x-ray of the spine is obtained with negative findings, the disorder is classified as non-specific. The next best step is to request an MRI with the appropriate enhancement for soft tissue inflammation. An experienced radiologist can identify any possible inflammatory conditions in the ligaments, discs, facet capsule or fascia. Once such inflammation is identified, the disorder could be excluded from the non-specific category as the indications of CTD are available.

CTD, to date, was considered as one of several types of non-specific low back pain, since its etiology was unknown. As such, a common treatment was exercise therapy with the objectives of preventing muscle atrophy, increasing the range of motion, strengthening the musculature, etc. The success rate resulting from such physical activities is near 50%, with the remaining patient population experiencing worsening conditions. CTD probably belongs to that group, since excessive physical activity was identified in this review as the source of the disorder. Prolonged rest (while continuing activities of daily living) for the lumbar spine is most likely the best option, as it allows the inflammation to finish its healing course without exposure to additional negative exposure.

Furthermore, a common treatment for acute inflammation is the administration of anti-inflammatory drugs. Considering that inflammation is a healing process, the use of such drugs could interfere, retard or even prevent the healing in the acute phase of the disorder. The use of pain medication could be a better alternative as it can provide comfort to the patient while allowing the completion of the healing process. It is still unclear how effective anti-inflammatory therapy could be to treat the disorder once it enters its chronic phase. Some research in this area can be extremely useful.

Other important implications on clinical treatment, for example, could be in manipulation therapy. Since it is now established that pro-inflammatory cytokines are responsible for triggering the cumulative syndrome, spinal manipulation therapy (SMT) may be used as a measure that can attenuate or block their expression level in the acute phase of the syndrome (Teodorczyk-Injeyan et al., 2006, 2008; Omos et al., 2009) and prevent the progression to the chronic phase. Additional techniques in manipulation therapy could be explored for optimal treatment of this disorder.

It should be emphasized that various personnel as well as workers should be trained to recognize symptoms of the acute phase and be alert to initiate the appropriate therapy or work rotation as soon as possible in order to prevent progression to the chronic phase. The chronic phase is a terminal degenerative stage, leaving little or no options for intervention (Leadbetter, 1990).

Finally, if the acute phase of inflammation progressed to the chronic phase and degeneration of the viscoelastic tissues took

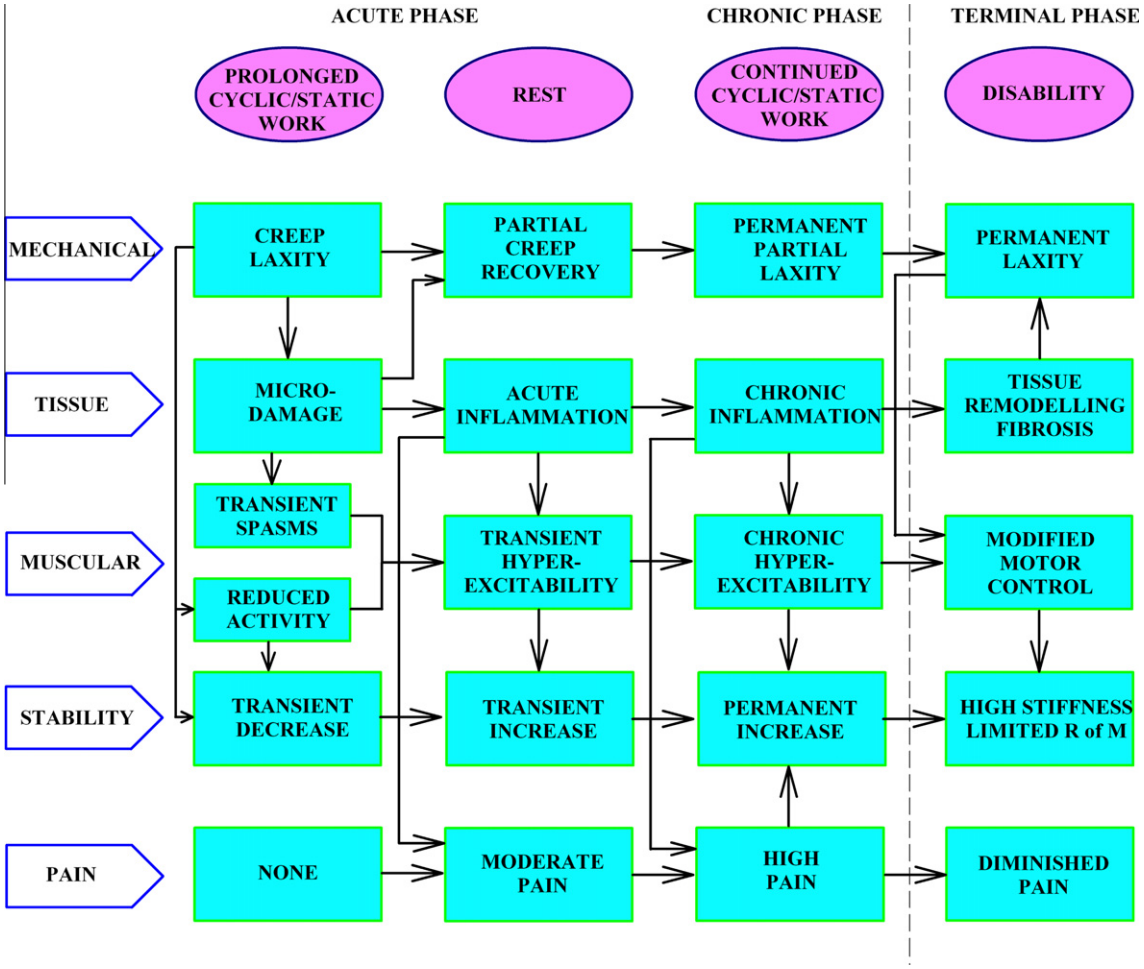

Fig. 14. Chart flow of the cumulative trauma syndrome development during the acute phase, as well as the progression into the chronic phase. The complex interactions of the various components are delineated over time.

place, fusion could be considered as a method to stabilize the spine and prevent the motor control components from limiting the range of motion, acting with inhibition such that weakness is present and generating pain. Such surgical procedure, however, has its risks and limitations that should be weighed carefully against the outcome. Fusion, by its definition, limits the range of motion and triggers changes in motor control that may not be always an improvement over the initial conditions.

5. Conclusions

The primary conclusions of this review point out that CTD is a complex multi-factorial syndrome! The major components of the syndrome consist of long lasting viscoelastic creep, profound changes in neuromuscular activity, stability and inflammation. Significant and complex time dependent interaction exists among the four components. Together, the "big picture" of the acute phase of cumulative disorder is obtained, demonstrating the complexity of this disorder and justifying its designation as a syndrome.

The major findings of this project consist of the following interactive factors:

1. High magnitude loads, long loading durations, large number of repetitions, high movement velocities and short rest periods in-between work sessions are high risk factors for CTD.
2. Of the several risk factors listed above, the most prominent one is high cyclic loading frequency, e.g. flexion at a high speed. This emerged from several perspectives.
3. Low magnitude loads, short loading durations, long in-between rest, low movement velocity and low number of repetitions were not found to constitute significant risk factor, yet demonstrated pronounced changes in creep, neuromuscular activity, stability and pro-inflammatory degradation. It would be more appropriate to designate these conditions as low risk factors.
4. Most importantly, the source of the cumulative disorder was found to be inflammation of the viscoelastic tissues of the lumbar spine, e.g. the tissue of failure are the ligaments and the mode of failure is inflammation.

In perspective, cumulative disorder is a rather complex multifactorial syndrome consisting of biomechanical, neuromuscular, tissue biology and stability components undergoing interactive, complex changes during the multiple phases of the loading and many hours of rest following the activity period. With the insight provided by this research program, diagnostic, preventive and treatment measures could be developed from the ergonomic/work planning phase to development of manipulation and pharmaceutical therapies that prevent the chronic phase.

Acknowledgments

This work was supported by NIOSH Grants RO1-OH-04079 and RO1-OH-07622 from the Centers for Disease Control and Prevention, The Occupational Medicine Research Center grant from The Louisiana Board of Regents and by the AEF from the School of Medicine, University of Colorado, Denver. The author wishes to express

his gratitude to his close team members of over 27 years, Drs. Bing He Zhou and Yun Lu. The author also wishes to acknowledge the contributions and collaboration of his associates; Drs. A. Gedalia, L. Espinoza, A. Zieske, R. Baratta, K. B. King and N. Banda and his many graduate students, residents and fellows who enriched the project during their training in neuro-musculoskeletal research in the Bioengineering Laboratory in New-Orleans and the Musculoskeletal Disorders Research Laboratory in Denver.

References

Andersson G. The epidemiology of spinal disorders. 2nd ed. Philadelphia: Lippincot-Raven; 1997.

Azar N, Kallakuri S, Chen C, Cavanaugh J. Strain and load thresholds for cervical muscle recruitment in response to quasistatic tensile loading of the caprine C5–C6 facet joint capsule. J Electromyogr Kinesiol 2009;19:e387–94.

Ben-Masaud A, Solomonow D, Davidson B, Zhou B, Lu Y, Patel V, et al. Motor control of lumbar instability following exposure to various cyclic load magnitudes. Eur Spine J 2009;18:1022–34.

Bove GM, Ransil BJ, Lin H-C, Leem JG. Inflammation induces ectopic mechanical sensitivity in axons of nociceptors innervating deep tissues. J Neurophysiol 2003;90:1949–55.

Cao DY, Khalsa P, Pickar J. Dynamic responsiveness of lumbar paraspinal muscle spindles during vertebral movement in cat. Exp Brain Res 2009;197:369–77.

Cavanaugh J, Lu J, Chen C, Kallakuri S. Pain generation in lumbar and cervical facet joints. J Bone Joint Surg Am 2006;88:63–7.

D'Ambrosia P, King K, Davidson B, Zhou B, Lu Y, Solomonow M. Increase pro-inflammatory cytokines in lumbar ligaments following low and high magnitudes cyclic loading. Eur Spine J 2010;19:1330–9.

Dickey J, McNorton S, Potvin J. Repeated spine flexion modulates the flexion-relaxation phenomenon. Clin Biomech 2003;18:783–9.

Dilley A, Bove GM. Resolution of inflammation induced axonal mechanical sensitivity and conduction slowing in C-fiber nociceptors. J Pain 2008;9(2):185–92.

Eversull E, Solomonow M, Zhou B, Baratta R, Zhu M. Neuromuscular neutral zones sensitivity to lumbar displacement rate. Clin Biomec 2001;16:102–13.

Fung D, Wang V, Laudier D, Shine J, Basta-Pljakic J, Jepesen K, et al. Subrupture tendon fatigue damage. J Orthop Res 2009;27:264–73.

Granata K, Marras W, Davis K. Variation in spinal load and trunk dynamics during repeated lifting exertions. Clin Biomech 1999;14:367–75.

Granata KP, Rogers E, Moorhouse K. Effects of static flexion-relaxation on paraspinal reflex behavior. Clin Biomech 2005;20:16–24.

Hendershoot B, Bazragari B, Muslim K, Toosizadeh N, Nussbaum M, Madigan M. Disturbance and recovery of trunk stiffness and reflexive muscle response following prolonged trunk flexion; influences of flexion angle and duration. Clin Biomech 2011;26:250–6.

Hoogendoorn WE, Bongers PM, de Vet HC, et al. Flexion and rotation of the trunk and lifting at work are risk factors for low back pain: results of a prospective cohort study. Spine 2000;25:3087–92.

Hoops H, Zhou B, Lu Y, Solomonow M, Patel V. Short rest between cyclic flexion periods is a risk factor for lumbar disorder. Clin Biomech 2007;22:745–57.

Ianuzzi A, Pickar J, Khalsa P. Determination of torque limits for human and cat lumbar spine specimens during displacement controlled physiological methods. Spine J 2009;9:77–86.

Ianuzzi A, Pickar JG, Khalsa PS. Validation of the cat as a model for human lumbar spine during simulated high-velocity, low amplitude spinal manipulation. J Biomech Eng 2010;132(7):071008.

Indahl A, Kaigle A, Reikeras O, Holm S. Electromyographic response of the porcine multifidus musculature after nerve stimulation. Spine 1995;20:2652–8.

Karajcarski S, Wells R. The time variation pattern of mechanical exposure and the reporting of low back pain. Theor Issues Ergon Sci 2006;1:27.

King K, Davidson B, Zhou B, Lu Y, Solomonow M. High magnitude cyclic load triggers inflammatory response in lumbar ligaments. Clin Biomech 2009;24:792–8.

Kumar S. Theories of musculoskeletal injury causation. Ergonomics 2001;44:17–47.

Kumar S. Biomechanics in ergonomics. Boca Raton, Fl, USA: CRC press; 2008.

Kumar S, Prasad N. Torso muscles EMG profile differences between patients of back pain and control. Clin Biomech 2010;25:103–9.

Le P, Solomonow M, Zhou B, Lu Y, Patel V. Cyclic load magnitude is a risk factor for cumulative low back disorder. J Occup Environ Med 2007;49:375–87.

Leadbetter W. An introduction to sports induced soft tissue inflammation. In: Leadbetter W, Buckwalter J, Gordon S, editors. Sports induced inflammation; clinical and basic science concepts. Park Ridge, IL, USA: Am. Acad. Orthopedic Surgeons; 1990.

Li L, Patel N, Solomonow D, Le P, Hoops H, Gerhardt D, et al. Neuromuscular response to cyclic lumbar twisting. Human Factors 2007;49:820–9.

Little J, Khalsa P. Human lumbar spine creep during cyclic and static flexion: creep rate, biomechanics, and facet joint capsule strain. Ann Biomed Eng 2005;33:391–401.

Lu D, Solomonow M, Zhou B, Baratta R, Li. Frequency dependent changes in neuromuscular response to cyclic lumbar flexion. J Biomech 2004;37:845–55.

Lu D, Davidson B, Zhou B, Lu Y, Patel V, Solomonow M. High frequency cyclic flexion is a risk factor for a lumbar disorder. Muscle Nerve 2008;38:867–74.

Marras WS. Occupational low back disorder causation and control. Ergonomics 2000;43:880–902.

McGill S, Brown S. Creep response of the lumbar spine to prolonged full flexion. Clin Biomech 1992;17:43–6.

McLain R, Pickar J. Mechanoreceptor endings in human thoracic and lumbar facet joints. Spine 1998;23:168–73.

Mountcastle V. Medical physiology. 13th ed. St. Louis: CV Mossby; 1974.

Navar D, Zhou B, Lu Y, Solomonow M. High repetition of cyclic loading is a risk factor for lumbar disorders. Muscle Nerve 2006;34:614–22.

Olson M, Li L, Solomonow M. Flexion-relaxation response to cyclic lumbar flexion. Clin Biomech 2004;19:769–76.

Olson M, Solomonow M, Li L. Flexion-relaxation response to gravity. J Biomech 2006;39:2545–54.

Olson M, Li L, Solomonow M. Interaction of viscoelastic tissue compliance with lumbar muscles during passive cyclic flexion-extension. J Electromyogr Kinesiol 2009;19:30–8.

Omos G, Mehrishi J, Bakacs T. Reduction in high blood TNF-α levels after manipulative therapy in 2 cervicogenic headache patients. J Manipulative Physiol Ther 2009;32(7):586–91.

Orchard J, James T, Portus M, Kountouris, Dennis R. Fast bowlers in cricket demonstrate up to 3–4 weeks delay between high workloads and increased risk of injury. Am J Sports Med 2009;37:1186–92.

Panjabi M, Goel V, Takata K. Physiologic strains in the lumbar spinal ligaments. Spine 1982;7:192–203.

Panjabi M, Courtney T. High speed sub failure stretch of rabbit ACL; changes in elastic failure and viscoelastic characteristics. Clin Biomech 2001;16:334–40.

Pickar J. An in vivo preparation for investigating neural responses to controlled loading of a lumbar vertebra in the anesthetized cat. J Neurosci Methods 1999;89:87–96.

Pinski S, King K, Zhou B, Lu Y, Davidson B, Solomonow M. High frequency loading of lumbar ligaments increases pro-inflammatory cytokines expression in a feline model of repetitive musculoskeletal disorder. Spine J 2010;10:1078–85.

Punnett L, Fine J, Keyserling M, et al. Back disorders and non neutral trunk postures of automobile assembly workers. Scand J Work Environ Health 1991;17:337–46.

Punnett L, Wegeman D. Work related musculoskeletal disorders; the epidemiologic evidence and the debate. J Electromyogr Kinesiol 2004;14:13–23.

Sanchez-Zuriaga D, Adams M, Dolan T. Is activation of back muscles impaired by creep or muscle fatigue. Spine 2010;35:517–25.

Shin G, Mirka G. An in vivo assessment of the low back response to prolonged flexion; interplay between active and passive tissues. Clin Biomech 2007;22:965–71.

Silverstein B, Fine L, Armstrong T. Hand wrist cumulative trauma disorders in industry. Br J Ind Med 1986;43:779–84.

Smit TH. The use of quadruped as an in vivo model for the study of the spine Biomechanical considerations. Eur Spine J 2002;11:137–44.

Smoljanovic T, Bojnic I, Hannafin J, Hren D, Delimar D, Pecina M. Traumatic and overuse injuries among international elite junior rowers. Am J Sports Med 2009;37:1193–9.

Solomonow M, Baten C, Smit J, Baratta RV, Hermens H, D'Ambrosia R, et al. EMG power spectra frequencies associated with motor unit recruitment strategies. J Appl Physiol 1990;68:1177–85.

Solomonow M, Zhou B, Harris M, Lu Y, Baratta R. The ligamento-muscular stabilizing system of the spine. Spine 1998;23:2552–62.

Solomonow M, Zhou B, Baratta R, Lu Y, Harris M. Biomechanics of increased exposure to lumbar injury due to cyclic loading: L loss of reflexive muscular stabilization. Spine 1999;24:2426–34.

Solomonow M, Zhou B, Baratta R, Lu Y, Zhu M, Harris M. Bi-exponential recovery model of lumbar viscoelastic creep and reflexive muscular activity after prolonged cyclic loading. Clin Biomech 2000;15:167–75.

Solomonow M, Eversull E, Zhou B, Baratta R, Zhu M. Neuromuscular neutral zones associated with viscoelastic hysteresis during cyclic lumbar flexion. Spine 2001;26:E-314–24.

Solomonow M, Baratta R, Zhou B, Burger E, Zieske A, Gedalia A. Muscular dysfunction elicited by creep of lumbar viscoelastic tissues. J Electromyogr Kinesiol 2003;13:381–96.

Solomonow M. Ligaments: a source of work related musculoskeletal disorder. J EMG Kinesiol 2004;14:49–60.

Solomonow D, Davidson B, Zhou B, Lu Y, Patel V, Solomonow M. Neuromuscular neutral zones response to cyclic lumbar flexion. J Biomech 2008;41:2821–8.

Stubbs M, Harris M, Solomonow M, Zhou B, Lu Y, Baratta R. Ligamento-muscular protective reflex in the spine. J Electromyogr Kinesiol 1998;8:197–204.

Teodorczyk-Injeyan J, Injeyan S, Ruegg R. Spinal manipulation therapy reduces inflammatory cytokines but not substance P production in normal subjects. J Manipulative Physiol Ther 2006;29:14–21.

Teodorczyk-Injeyan J, Injeyan S, McGregor M, Harris G, Ruegg R. Enhancement of in-vitro interlukin -2 production in normal subjects following a single spinal manipulative treatment. Chiropractic Osteopathy 2008;16(5):1–9.

van Dieen J, Selen L, Cholewicki J. Trunk muscle activation in low-back pain patients; an analysis of the literature. J Electromyogr Kinesiol 2003;13:333–51.

Wang X, Hamza M, Wu T, Dionne R. Upregulation of IL-6, IL-8 and CCL2 gene expression after acute inflammation: correlation to clinical pain. Pain 2009;142:275–83.

Williams M, Solomonow M, Zhou B, Baratta V, Harris M. Multifidus spasms elicited by prolonged lumbar flexion. Spine 2000;25:2916–24.

Wilke HJ, Kettler A, Claes L. Are sheep spines a valid biomechanical model for human spines? Spine 1997;22:2365–74.
Woo S, Gomez M, Amiel D, Akeson W. The effect of exercise on the biomechanical and biochemical properties of swine digital flexor tendon. J Biomech Eng 1981;103:51–6.
Woo S, Gomez M, Woo Y, Akeson W. Mechanical properties of tendons and ligaments; the relationships of exercise in tissue remodeling. Biorheology 1982;19:379–408.
Woo S, Apreleva M, Hoher J. Tissue mechanics of ligaments and tendons. In: Kumar S, editor. Biomechanics in ergonomics. London, UK: Taylor & Francis; 1999.
Yang G, Marras W, Best T. The biochemical response to biomechanical tissue loading on the low back during physical work exposure. Clin Biomech 2011;26:431–7.

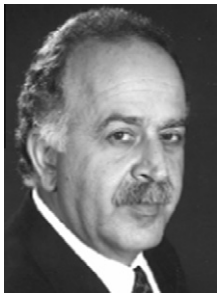

Dr. Moshe Solomonow is Professor and Director of the Bioengineering Division and of the Musculoskeletal Disorders Research Laboratory in the Department of Orthopedics at the University of Colorado Health Sciences Center in Denver. He was a Professor and Director of Bioengineering and of The Occupational Medicine Research Center at Louisiana State University Health Sciences Center in New Orleans, Louisiana from 1983 to 2005.

He received the B.Sc., and M.Sc. in Electrical Engineering from California State University and the Ph.D. in Engineering Systems and Neuroscience from the University of California, Los Angeles,1976.

Under his leadership, technology was developed for several translational projects related to; Myoelectric control of upper limb prosthetics for amputees; Electronic walking orthosis for paraplegics; Smart orthosis for Anterior Cruciate Ligament deficient patients; and smart braces for individuals with low back pain.

He is the Founding Editor of The *Journal of Electromyography and Kinesiology*, and served on the Editorial Board of several bioengineering and medical journals. Dr. Solomonow is/was a consultant to the National Science Foundation, National Institutes of Health, Centers for Disease Control, National Academy of Sciences, The Veterans Administration and scientific agencies of several European and Asiatic governments and Canada. He was a council member of the International Society of Electrophysiological Kinesiology, the International Society of Functional Electrical Stimulation, and the IEEE-Biomedical Engineering Society. He published over 150 refereed journal papers on musculoskeletal disorders including: Motor Control, Electromyography, Muscle, Tendon, Ligament and Joint Biomechanics, Electrical Muscle Stimulation, Orthotic systems for Paraplegic locomotion, Low Back Disorders and Knee Injury.

He supervised more than 150 engineering, physical therapy, kinesiology, physiology, medical students and orthopedic residents, as well as postgraduate students and fellows from several countries.

Dr. Solomonow organized the EMG Tutorial Workshop in the ISB Congress, the Canadian Society of Biomechanics, The Human Factors and Ergonomics Society, and The Society for Clinical Movement Analysis, was on the organizing committee of numerous conferences and gave keynote and symposia lectures in many others. He received the Crump Award for Excellence in Bioengineering Research (UCLA), the Distinctive Contribution Award from Delta 7 Society (France), The Doctor Medicine Honoris Causa (Vrije Universitiet, Brussels), The I. Cahen Professorship (LSUHSC) and the 1999 Volvo Award for Low Back Pain Research.